# Norton Sound red king crab stock assessment

Appendix D: spatiotemporal model-based abundance index

Caitlin Stern[1,2]
[1]Alaska Department of Fish and Game
[2]caitlin.stern@alaska.gov

May 2026

## Summary

The Norton Sound red king crab (*Paralithodes camtschaticus*) stock assessment uses estimated abundance from three fishery-independent surveys as indices of abundance in the stock assessment model: the historical National Oceanic and Atmospheric Administration (NOAA) Norton Sound trawl survey, the NOAA Northern Bering Sea (NBS) trawl survey, and the Alaska Department of Fish and Game (ADF&G) Norton Sound trawl survey. These surveys cover different years and areas, and within a survey the set of locations sampled sometimes varies among years, meaning that annual estimates may not be directly comparable. While the complete lack of overlap in time means that the historical Norton Sound trawl survey cannot be combined with the other two surveys in a single model, the two ongoing surveys have both spatial and temporal overlap. Using a spatiotemporal modeling approach to combine the NBS and ADF&G survey data into a single index of abundance for inclusion in the stock assessment model offers the opportunity to produce directly comparable annual estimates of abundance, potentially improving the reliability of the abundance time series. This document details the development of a spatiotemporal model-based abundance index which will be included in proposed NSRKC stock assessment model runs presented at the Crab Plan Team meeting in May 2026.

## Introduction

Indices of abundance are key inputs to stock assessment models, providing information crucial for estimating stock size (Patterson et al. 2001; Maunder and Punt 2004). However, design-based methods for producing these indices from fishery-independent surveys can yield biased results when practical constraints lead survey sampling to deviate from survey design. For example, financial resources may not be sufficient for surveys to occur as frequently as planned, or changes in survey priorities may limit vessels to sampling only a subset of survey stations. Spatiotemporal models including spatial and spatiotemporal random effects have the potential to mitigate the effects of inconsistent survey sampling by accounting for the spatiotemporal processes that underlie survey observations (Thorson et al. 2021; Yalcin et al. 2023). Simulation work suggests than index standardization using well-specified spatiotemporal models can reduce the impact of changes in survey effort by providing a consistent method of inferring abundance in missing areas (Yalcin et al. 2023).

In addition to suffering from bias due to changes in survey sampling, design-based indices of abundance can inflate temporal variability by failing to account for spatial dependence (Shelton et al. 2014; Thorson et al. 2015). Due to the importance of indices of abundance in stock assessment models, this can lead to increased uncertainty in outputs used in fishery management (Cao et al. 2017). By accounting for spatial variation in survey catch, as well as incorporating habitat variables, spatiotemporal model-based index

standardization can produce abundance indices with reduced variability compared to design-based indices (Cao et al. 2017, Chen et al. 2024). This can lead to less extreme retrospective patterns for stock assessment models that use model-based rather than design-based indices (Cao et al. 2017, Chen et al. 2024).

The population of red king crab (*Paralithodes camtschaticus*) in Norton Sound, Alaska, supports locally important commercial and subsistence fisheries. The stock assessment for Norton Sound red king crab uses three fishery-independent trawl survey time series in design-based indices of abundance: the NOAA Norton Sound trawl survey (1976 - 1991), the ADF&G Norton Sound trawl survey (1996 - present), and the NOAA NBS trawl survey (2010 - present) (Stern and Palof 2025; Hamazaki 2024). The data sets from these surveys, all of which use a systematic sampling design, cover different years and spatial footprints, and within a survey the set of locations sampled sometimes varies among years (Figure 1). This history of both spatial and temporal variation in survey sampling is one of the factors motivating the development of spatiotemporal model-based indices for this stock, as standardization over both space and time is required.

Initial work on a model-based approach for deriving Norton Sound red king crab survey indices of abundance led to the development of three separate model-based indices of abundance, one for each of the survey time series (Stern 2025). However, replacing the design-based indices of abundance with these model-based indices of abundance in the stock assessment model did not seem to improve key aspects of the stock assessment model, including the retrospective pattern (Stern and Palof 2025). Combining data from the two ongoing surveys into a single model-based index of abundance has been a long-standing goal for this stock assessment, and seemed the logical next step given the lack of improvement following the incorporation of separate model-based indices. This document details the development of a spatiotemporal model-based abundance index combining data from the NBS and ADF&G trawl surveys; this index will be evaluated for inclusion in the 2026 NSRKC stock assessment.

# Methods

## Data sources

I used the R (R Core Team 2026) package **crabpack** (Hennessey 2025) to extract the NOAA NBS trawl survey data (2010 - 2025). I obtained the ADF&G trawl survey data (1999 - 2024) from Jenifer Bell of ADF&G. Survey effort is displayed in Figure 1. The ADF&G and NBS surveys have taken place in the same year four times: 2017, 2019, 2021, and 2023. For both surveys, I calculated crab density at a survey station as the number of male red king crab $\geq$ 64 mm in carapace length (CL) at the station divided by the area swept in $km^2$. Three different visualizations of these data are shown in Figures 2 - 4. Figure 2 illustrates the changes across the time series in both survey station sampling and the set of survey stations at which at least one male red king crab $\geq$ 64 mm in CL was recorded. Red king crab are consistently detected within a core area in Norton Sound, and are occasionally detected in areas to the north or south of the core area. Figure 3 shows crab density at each survey station. Figure 4 shows the same information as Figure 3, but with crab density represented using point color rather than point size, making it easier to determine at which survey stations the highest crab densities were recorded.

## Spatiotemporal models

I fit geostatistical GLMMs with spatiotemporally correlated random effects to survey data using the R package **sdmTMB** (Anderson et al. 2022). In this approach, spatial effects are modeled using the stochastic partial differential equation (SPDE) approximation to Gaussian random fields (Lindgren et al. 2011). The rate at which spatial covariance decays with distance is defined by the Matèrn covariance function, a derived parameter of which is the spatial (or Matèrn) range, the distance at which spatial correlation decays such that two points are effectively independent (Anderson et al. 2022). **sdmTMB** uses geostatistical time series data to estimate spatial and spatiotemporal generalized linear mixed effects models (GLMMs). This approach allows for index standardization when the set of stations surveyed is not consistent across years: one can

generate a spatial grid that covers the area of interest, predict from the model onto that grid, and sum the predicted abundance to obtain an area-weighted index that is independent of sampling locations (Anderson et al. 2022).

Applying the SPDE approach to modeling random fields requires defining a triangulation mesh of the spatial domain (Anderson et al. 2022). I constructed a triangulation mesh for the combined NBS and ADF&G survey data set using the **sdmTMB** function make_mesh(), a wrapper for the triangulation mesh functions in the **fmesher** package (Lindgren 2023), and the **sdmTMBextra** (Anderson 2025) function add_barrier_mesh(). The add_barrier_mesh function permitted incorporation of correlation barriers based on the Norton Sound coastline. The resulting mesh is shown in Figure 5. Figure 6 shows the vertices included (black circles) versus excluded (red crosses) from the mesh, demonstrating that the barrier mesh approach effectively excluded from the mesh both vertices on land and vertices outside of the designated spatial polygon.

For all models, I estimated spatiotemporal random fields as independent and identically distributed (IID). The spatial random fields are estimated for each time slice, the period of which is specified in the model (e.g., time = year). Estimating spatiotemporal random fields as IID is likely most appropriate for the standardization of survey indices intended to be used in stock assessment models as this approach minimizes the estimation covariance among years, which is usually ignored in stock assessment models (Thorson et al. 2020, Chen et al. 2024). I compared models in which the only fixed effects were year and survey (NBS or ADF&G), specified as factors, with models that also included survey station depth (m) as a covariate, as variation in the depth of stations surveyed from year to year could influence estimated abundance if not taken into account. Depth was centered and scaled by its standard deviation. I ran models with the Tweedie, delta gamma, and delta lognormal distribution families.

## Model evaluation and diagnostics

After fitting models, I checked model convergence using the **sdmTMB** sanity() function. Models were considered converged if they met the following criteria evaluated by the sanity() function: the non-linear minimizer suggested successful convergence, the Hessian matrix was positive definite, no extreme or very small eigenvalues were detected, all gradients with respect to fixed effects were $< 0.001$, no fixed-effect standard errors were NA, no standard errors looked unreasonably large, no sigma parameters were $< 0.01$; no sigma parameters were $> 100$, and the range parameter was of a reasonable size. Models that did not converge were excluded from further consideration.

For models that passed all the sanity checks, I calculated residuals using the **DHARMa** package (Hartig 2024) and examined diagnostics included in the package. I plotted the DHARMa residuals over space and time to visualize potential patterns of autocorrelation.

I evaluated model predictive skill (the predictive ability of the model for new observations; Anderson *et al.* 2024) using the cross validation function sdmTMB_cv(). This function measures model predictive skill by holding out subsets of the data in turn and using each as a test set. These subsets of data are termed "folds". Following the practices of similar investigations (e.g., Vihtakari *et al.* 2026), I compared models by performing cross validation with 10 randomly arranged folds for each model before extracting the model's total predicted out-of-sample negative log-likelihood (NLL). The model with the smallest NLL was deemed the best-fitting model. I calculated Root Mean Square Error (RMSE) and Mean Absolute Error (MAE) based on the predictive values; smaller RMSE and MAE values indicate better model fit.

## Predictions

To generate a prediction grid, I pulled the NBS trawl survey stratum for NSRKC from the **akgfmaps** package (AFSC 2026; Figure 7) using the get_crab_strata() function, then produced a grid with a resolution of 5 $km^2$ that matched the NSRKC survey stratum area (Figure 8). The NBS survey stratum covers a smaller area than the spatial mesh used in model fitting and includes most but not all survey observations (Figure 9). I used the **sdmTMB** predict() function to generate predicted crab abundance from each model over

the prediction grid. In order to make predictions from models containing a depth covariate, I added depth information to the prediction grid using a georeferenced TIFF file from the Southern Alaska Coastal Relief Model (Lim et al. 2011).

### Indices of abundance

I used the **sdmTMB** get_index() function to calculate total abundance estimates and standard errors from each model, then plotted these model-based indices with the design-based indices currently used in the stock assessment model for visual comparison.

## Results

### Model diagnostics

I ran six models: one model with year and survey as fixed effects, and one model with year, survey, and depth as fixed effects, for each of the three distribution families (Tweedie, delta gamma, and delta lognormal). All six models converged and passed sanity checks.

Comparing diagnostics using DHARMa residuals among the models showed that the models performed similarly: all six models showed evidence of significant deviation in the dispersion test and no evidence of significant deviation in the outlier or Kolmogorov-Smirnov tests (Figures 10 - 15). The spatial distributions of residuals did not appear to show concerning patterning (Figures 16 - 21).

Cross-validation analysis for the delta lognormal distribution family models produced non-positive-definite Hessian matrices in 3 of 10 folds for the model without the depth covariate and 6 of 10 folds for the model with the depth covariate, so these models were excluded from further consideration. Among the models for which cross-validation analysis was successful, the model using the delta gamma distribution family with year, survey, and depth as fixed effects had the smallest NLL value, indicating that this model had the best out-of-sample predictive skill of the models evaluated; this model also had the second-smallest MAE and RMSE values (Figure 22). Based on these model selection criteria, the model using the delta gamma distribution family with year, survey, and depth as fixed effects is the best-fitting model and I used this model to generate the abundance estimates for the model-based index in the stock assessment model.

The Matèrn range for the presence/absence component of the best-fitting model was 121 km, indicating spatial autocorrelation in crab presence/absence over a large distance, while the range was smaller for the positive catch component of the model, indicating spatial autocorrelation in crab abundance over a shorter distance (Table 1). Standard deviations were higher for spatial fields ($\sigma_\omega$) than for spatiotemporal fields ($\sigma_\epsilon$) for the presence/absence model components, indicating that spatial variability was larger than spatiotemporal variability for crab presence/absence, while the opposite was true for the positive catch component of the model, indicating that spatial variability was smaller than spatiotemporal variability for crab abundance (Table 1). The fixed effect coefficient estimate for the NBS survey was positive in the delta gamma distribution models but negative in the Tweedie distribution models, while the estimate for scaled depth was positive in both models that included this fixed effect (Table 2).

### Model predicted abundance

The spatial distributions of model-predicted crab presence/absence and/or abundance for the models for which cross-validation analysis was successful are shown in Figures 23 - 28 and appear broadly concordant with spatial abundance patterns observed in the surveys (Figure 3).

### Model-based abundance indices compared to the design-based abundance indices

Abundance estimates from the design-based indices are shown alongside model-based estimates in Figures 29 and 30. For the models using the delta gamma distribution family, the spatiotemporal model-based abundance estimates tend to be smaller in scale than the design-based abundance estimates, particularly when the depth covariate is included (Figure 29); including depth similarly reduces the scale of abundance estimates for the models using the Tweedie distribution family (Figure 30). The model-based abundance estimates from the models using the delta gamma distribution family also show reduced interannual variability compared to the design-based estimates, a finding consistent with previous work (Cao et al. 2017, Chen et al. 2024).

## Conclusions

The spatiotemporal model-based abundance index for Norton Sound red king crab accounts for differences in survey stations sampled among years and across space, producing a consistent time series that includes data from both the NOAA NBS and ADF&G trawl surveys. This model-based abundance index will be evaluated for inclusion in the 2026 NSRKC stock assessment model.

## Acknowledgements

I thank the members of the North Pacific Fishery Management Council Crab Plan Team, as well as Chris Siddon and Alex Reich of ADF&G, for their helpful feedback on earlier versions of this work. I thank Lewis Barnett and Sean Hardison for providing invaluable advice on the development of the spatiotemporal models.

## References

Anderson SC (2025) sdmTMBextra: Extra Functions for Working with 'sdmTMB' Models. R package version 0.0.4, commit 63f236912e12ce78b5a0529eedf1e11cb93d0a10, https://github.com/pbs-assess/sdmTMBextra.

Anderson SC, Ward EJ, English PA, Barnett LAK (2022) sdmTMB: An R package for fast, flexible, and user-friendly generalized linear mixed effects models with spatial and spatiotemporal random fields. bioRxiv, *2022.03.24.485545*. doi:10.1101/2022.03.24.485545.

Anderson SC, Ward EJ, English PA, Barnett LAK, Thorson JT (2024) Cross-validation for model evaluation and comparison. Retrieved from https://pbs-assess.github.io/sdmTMB/articles/cross-validation.html.

Bivand RS. 2022. spdep: Spatial Dependence: Weighting Schemes, Statistics. R Package Version 1.2-1, https://CRAN.R-project.org/package=spdep.

Cao J, Thorson JT, Richards RA, Chen Y (2017) Spatiotemporal index standardization improves the stock assessment of northern shrimp in the Gulf of Maine. Canadian Journal of Fisheries and Aquatic Sciences 74: 1781–1793 doi:10.1139/cjfas-2016-0137.

Cacciapaglia C, Brooks EN, Adams CF, Legault CM, Perretti CT, Hart D (2024) Developing workflow and diagnostics for model selection of a vector autoregressive spatiotemporal (VAST) model in comparison to design-based indices. Fisheries Research 275:107009 doi:10.1016/j.fishres.2024.107009.

Chen J, Gao J, Zhang F (2024) Spatiotemporal model improves survey indices for witch flounder stock assessment in the Grand Banks. Canadian Journal of Fisheries and Aquatic Sciences 81:459–487 doi:10.1139/cjfas-2023-0101.

DeFilippo L, Kotwicki S, Barnett L, Richar J, Litzow MA, Stockhausen WT, Palof K (2023) Evaluating the impacts of reduced sampling density in a systematic fisheries-independent survey design. Frontiers in Marine Science 10:1219283 doi:10.3389/fmars.2023.1219283.

Hamazaki T (2024) Norton Sound red king crab stock assessment for the fishing year 2024. In: Stock Assessment and Fishery Evaluation Report for the King and Tanner Crab Fisheries of the Bering Sea and Aleutian Islands: 2024 Final Crab SAFE. North Pacific Fishery Management Council, Anchorage AK. PDF.

Hartig F (2024) DHARMa: Residual Diagnostics for Hierarchical (Multi-Level / Mixed) Regression Models. R package version 0.4.7, https://CRAN.R-project.org/package=DHARMa.

Hennessey S (2025) crabpack: Calculate Bering Sea Crab CPUE, Abundance, and Biomass. R package version 1.0.0, commit 65322a20b78cf157b69587eb3039e30ec8ee114d, https://github.com/AFSC-Shellfish-Assessment-Program/crabpack.

Lim E, Eakins BW, Wigley R (2011) Coastal Relief Model of Southern Alaska: Procedures, Data Sources and Analysis, NOAA Technical Memorandum NESDIS NGDC-43.

Moran PA (1950) Notes on continuous stochastic phenomena. Biometrika 37:17–23. doi:10.1093/biomet/37.1-2.17.

R Core Team (2026) R: A Language and Environment for Statistical Computing. R Foundation for Statistical Computing, Vienna, Austria. https://www.R-project.org/.

Shelton AO, Thorson JT, Ward EJ, Feist BE (2014) Spatial semiparametric models improve estimates of species abundance and distribution. Canadian Journal of Fisheries and Aquatic Sciences 71:1655–1666 doi:10.1139/cjfas-2013-0508.

Stern (2025) Spatiotemporal model-based survey indices of abundance for Norton Sound red king crab. North Pacific Fishery Management Council, Anchorage AK. PDF.

Stern and Palof (2025) Proposed models for the 2025 Norton Sound red king crab stock assessment. North Pacific Fishery Management Council, Anchorage AK. PDF.

Thorson JT, Cunningham CJ, Jorgensen E, Havron A, Hulson P-JF, Monnahan CC, von Szalay P (2021) The surprising sensitivity of index scale to delta-model assumptions: recommendations for model-based index standardization. Fisheries Research 233:105745. doi:10.1016/j.fishres.2020.105745.

Vihtakari M, Aune M, Assmann KM, Howell D, Hallfredsson EH, Ward EJ (2026) Demersal distribution and fisheries independent trends of beaked and golden redfish in the Barents and Norwegian Seas. ICES Journal of Marine Science 83:fsag009 doi:10.1093/icesjms/fsag009.

Yalcin S, Anderson SC, Regular PM, English PA (2023) Exploring the limits of spatiotemporal and design-based index standardization under reduced survey coverage. ICES Journal of Marine Sciences 80:2368-2379. doi:10.1093/icesjms/fsad155.

# Tables

Table 1: Spatial parameter estimates of the models for which cross-validation analysis was successful. Delta (hurdle) models include one component that models presence/absence and one component that models positive catch (abundance); results from both model components are shown. These models used either the delta gamma (DG) or Tweedie distribution families. Terms include the Matèrn range (the distance at which spatial correlation decays such that two points are effectively independent), the standard deviation for spatial fields ($\sigma_\omega$), and the standard deviation for spatiotemporal fields ($\sigma_\epsilon$).

| Distribution | Fixed effects | Component | Term | Estimate | SE |
|---|---|---|---|---|---|
| DG | year, survey | presence/absence | range | 114.85 | 30.88 |
| DG | year, survey | presence/absence | sigma_O | 1.78 | 0.35 |
| DG | year, survey | presence/absence | sigma_E | 0.35 | 0.17 |
| DG | year, survey | positive catch | range | 38.25 | 8.02 |
| DG | year, survey | positive catch | phi | 1.86 | 0.15 |
| DG | year, survey | positive catch | sigma_O | 0.60 | 0.11 |
| DG | year, survey | positive catch | sigma_E | 0.69 | 0.07 |
| DG | year, survey, depth | presence/absence | range | 120.60 | 31.21 |
| DG | year, survey, depth | presence/absence | sigma_O | 1.85 | 0.35 |
| DG | year, survey, depth | presence/absence | sigma_E | 0.31 | 0.18 |
| DG | year, survey, depth | positive catch | range | 41.42 | 8.81 |
| DG | year, survey, depth | positive catch | phi | 1.85 | 0.15 |
| DG | year, survey, depth | positive catch | sigma_O | 0.60 | 0.11 |
| DG | year, survey, depth | positive catch | sigma_E | 0.67 | 0.07 |
| Tweedie | year, survey | | range | 55.63 | 8.96 |
| Tweedie | year, survey | | phi | 32.45 | 1.84 |
| Tweedie | year, survey | | sigma_O | 1.46 | 0.22 |
| Tweedie | year, survey | | sigma_E | 1.10 | 0.10 |
| Tweedie | year, survey | | tweedie_p | 1.33 | 0.02 |
| Tweedie | year, survey, depth | | range | 58.20 | 9.18 |
| Tweedie | year, survey, depth | | phi | 32.28 | 1.85 |
| Tweedie | year, survey, depth | | sigma_O | 1.44 | 0.20 |
| Tweedie | year, survey, depth | | sigma_E | 1.11 | 0.10 |
| Tweedie | year, survey, depth | | tweedie_p | 1.31 | 0.02 |

Table 2: Estimates of the survey and scaled depth fixed effect coefficients from the models for which cross-validation analysis was successful. These models used either the delta gamma (DG) or Tweedie distribution families.

| Distribution | Fixed effects | Term | Estimate | SE |
|---|---|---|---|---|
| DG | year, survey | survey.fNBS | 0.77 | 0.30 |
| DG | year, survey, depth | survey.fNBS | 0.43 | 0.31 |
| DG | year, survey, depth | depth_scaled | 0.89 | 0.21 |
| Tweedie | year, survey | survey.fNBS | -0.18 | 0.18 |
| Tweedie | year, survey, depth | survey.fNBS | -0.42 | 0.18 |
| Tweedie | year, survey, depth | depth_scaled | 0.80 | 0.13 |

## Figures

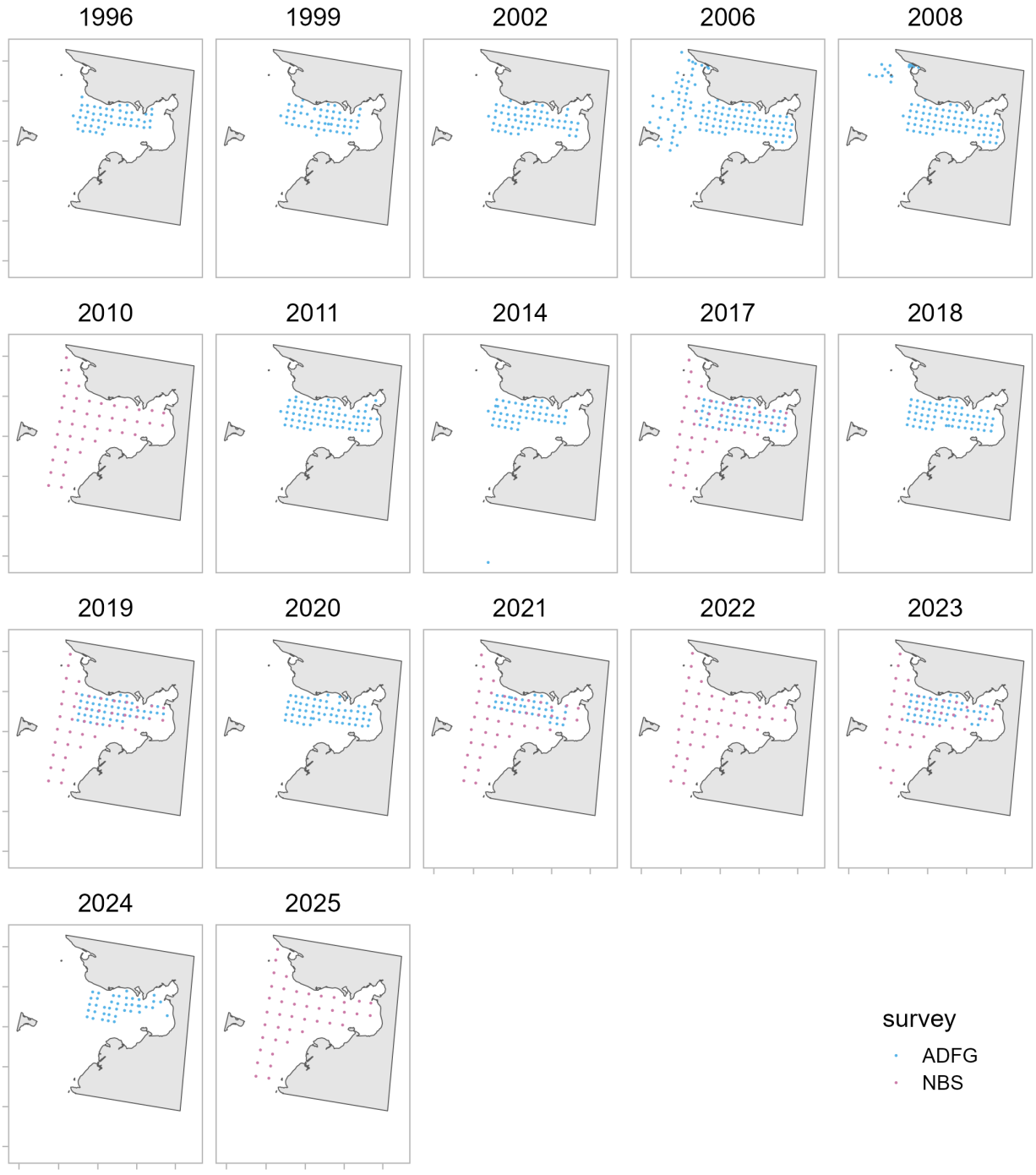


Figure 1: Norton Sound red king crab survey stations sampled in each year of the Northern Bering Sea (NBS; pink points) and Alaska Department of Fish and Game (ADFG; blue points) trawl survey time series. Note the variation in the set of survey stations sampled in each year.

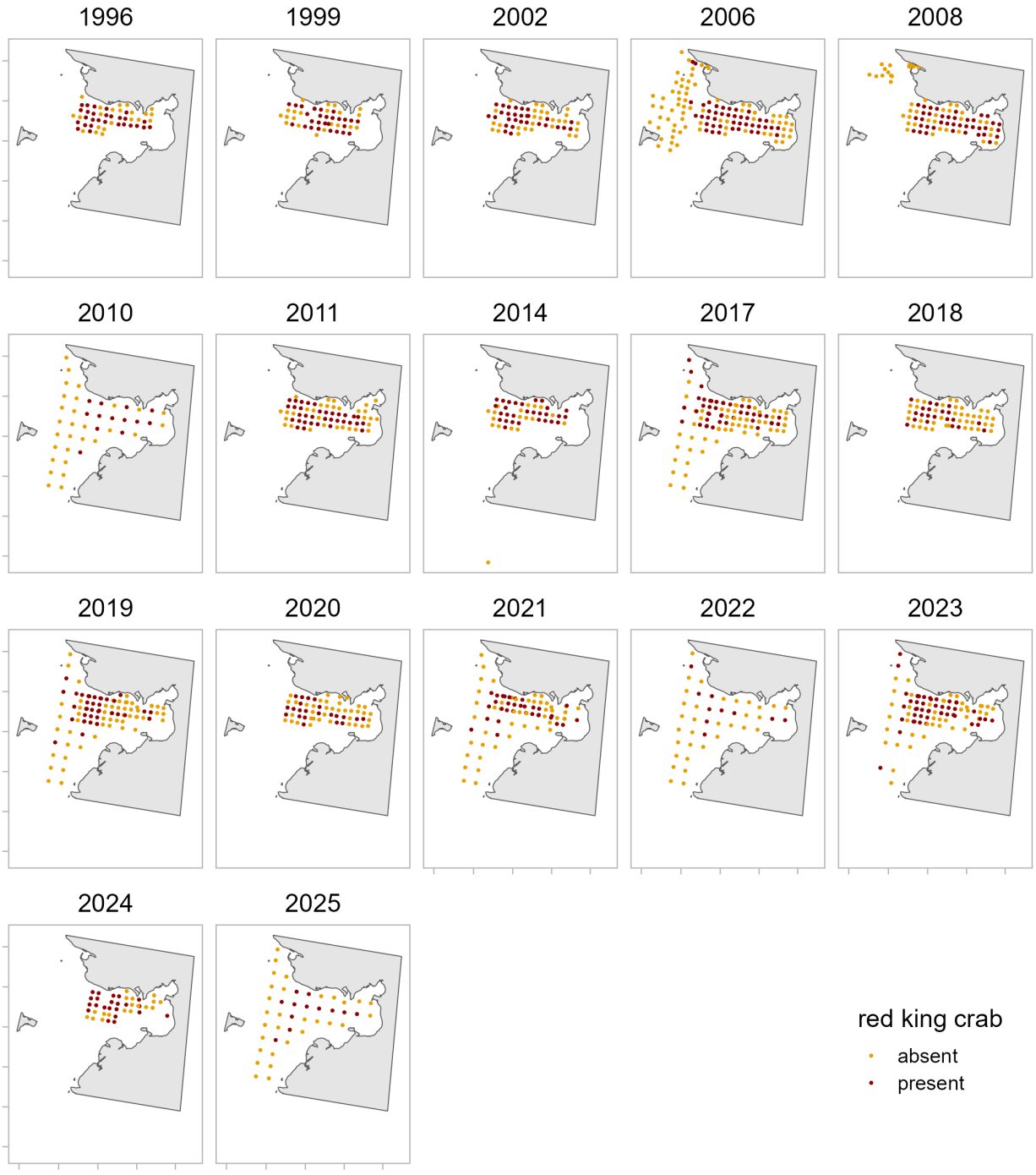


Figure 2: Presence and absence of Norton Sound red king crab at sample survey stations. Stations colored orange recorded no male red king crab $\geq$ 64 mm in carapace length, while stations colored red recorded at least one male red king crab $\geq$ 64 mm in carapace length.

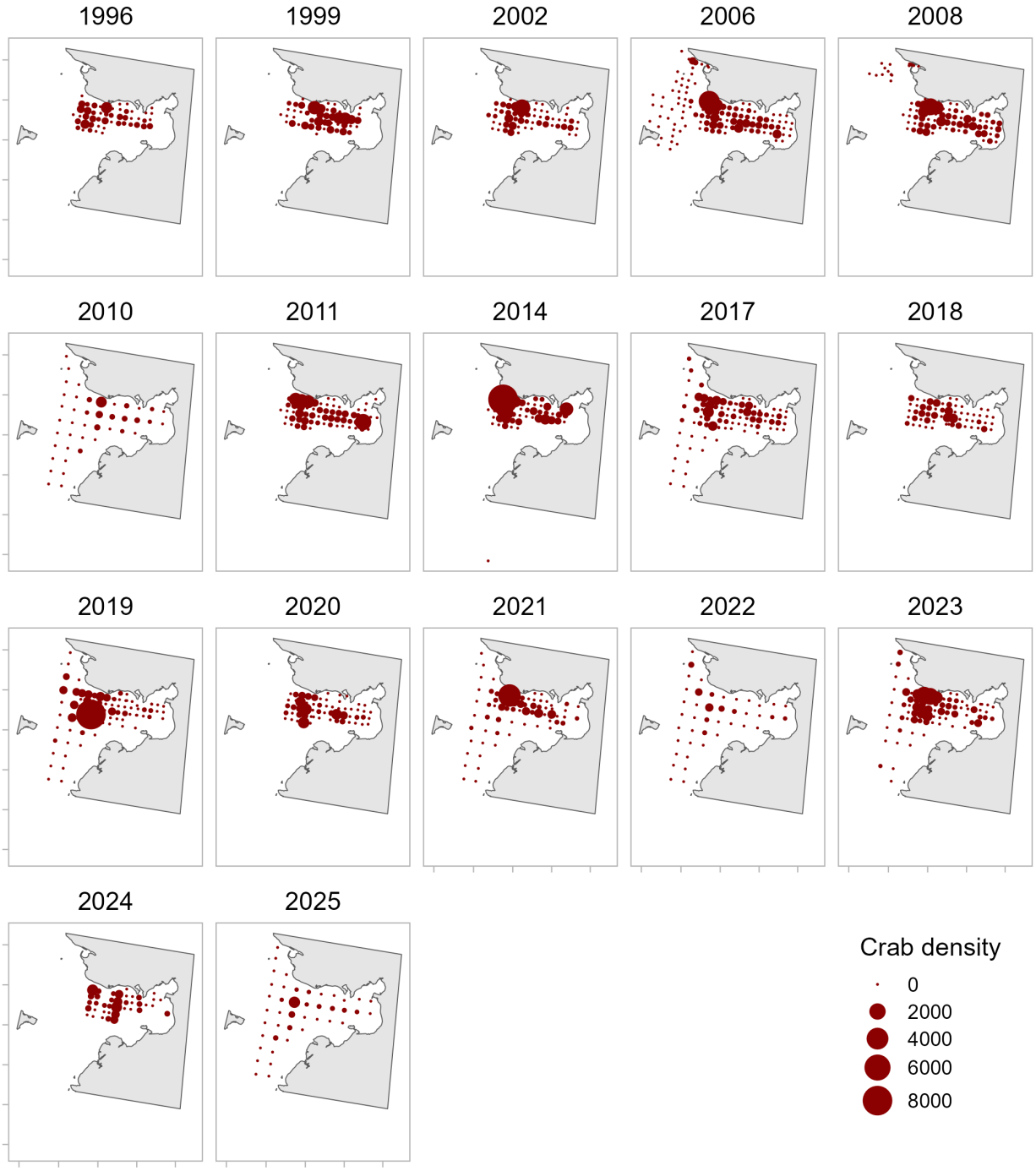


Figure 3: Norton Sound red king crab density at survey stations sampled in each year. Point size is proportional to the density of male red king crab $\geq$ 64 mm in carapace length at the station.

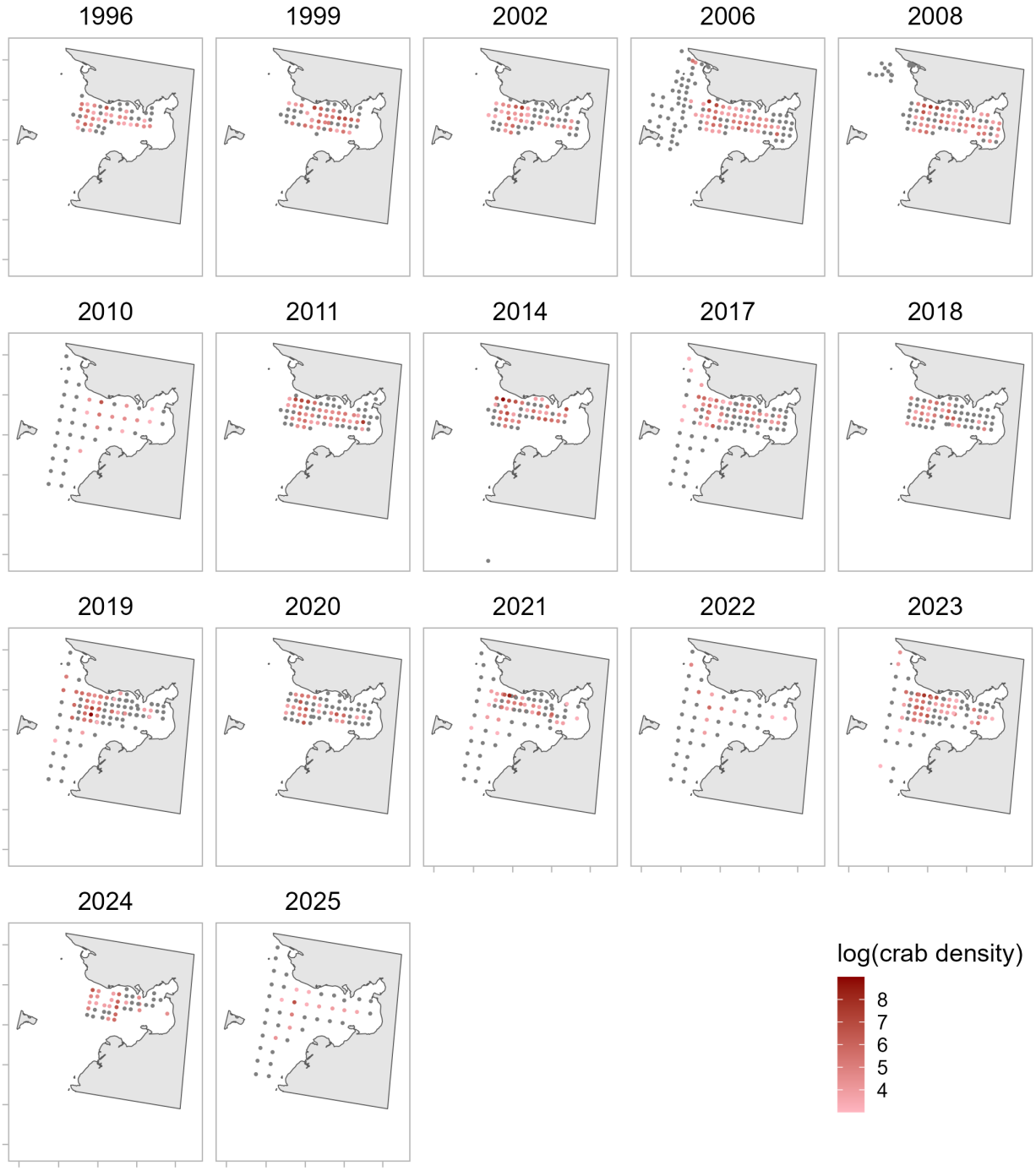


Figure 4: Norton Sound red king crab density at survey stations sampled in each year. Point color is proportional to the density of male red king crab $\geq$ 64 mm in carapace length at the station.

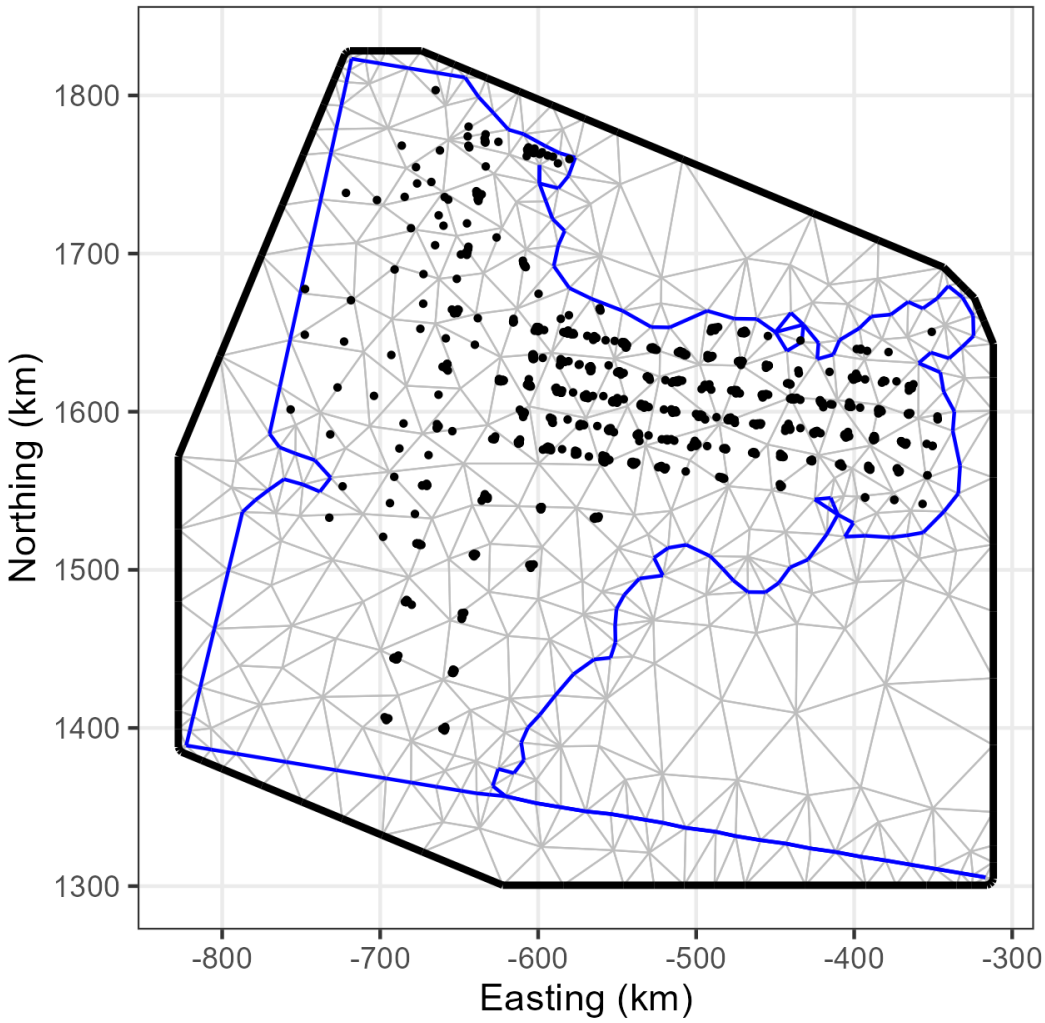


Figure 5: Spatial mesh used in spatiotemporal models, with ADFG and NOAA NBS survey observations shown as black points. The blue line shows the land and polygon boundaries used to delineate which vertices to include in the mesh. Vertices on land or outside the designated polygon were excluded from the mesh.

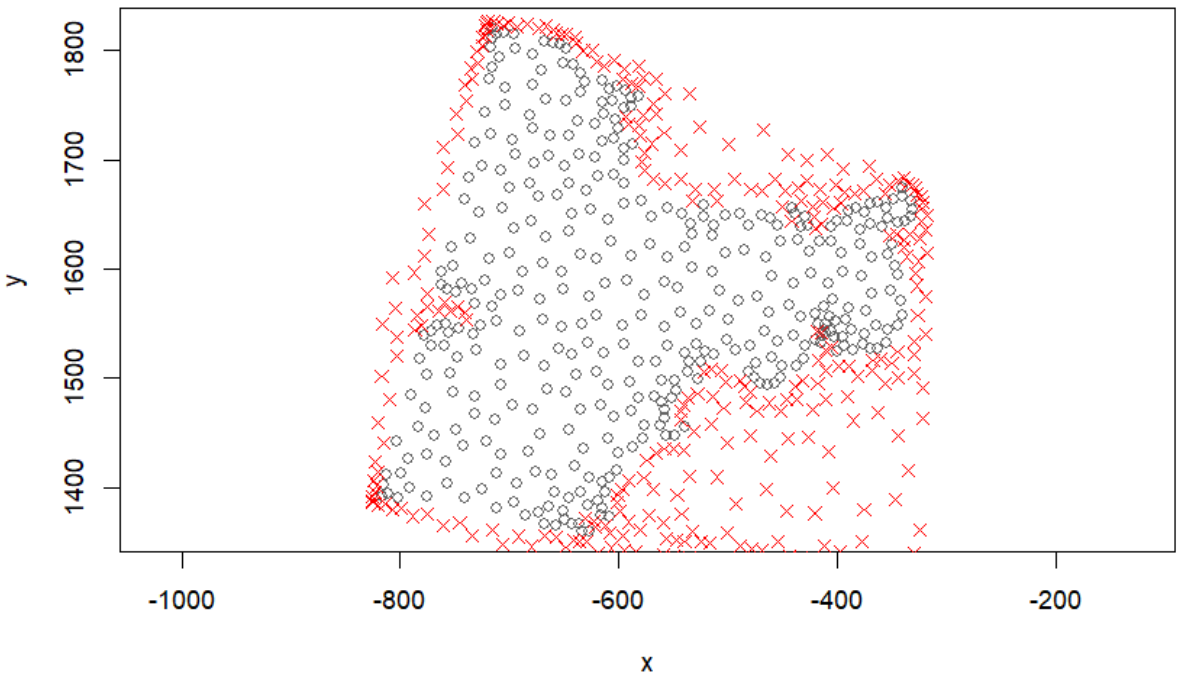


Figure 6: Vertices of the spatial barrier mesh used in spatiotemporal models, demonstrating that land as well as the area outside the designated polygon are excluded from the mesh (red crosses).

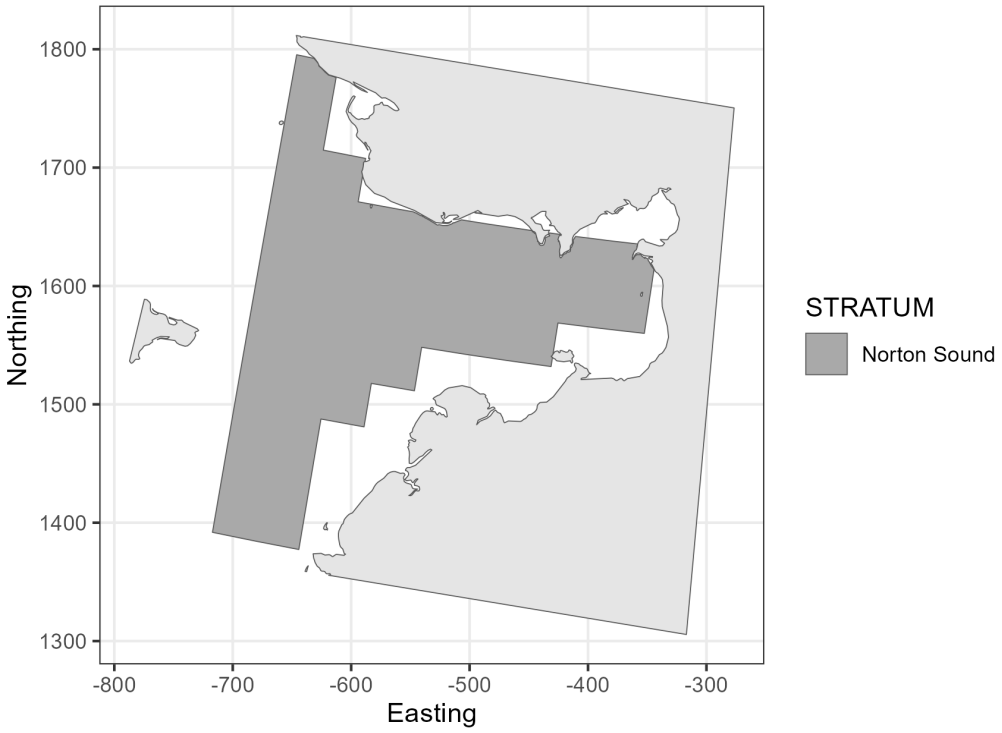


Figure 7: NOAA Northern Bering Sea bottom trawl survey stratum for the Norton Sound red king crab stock.

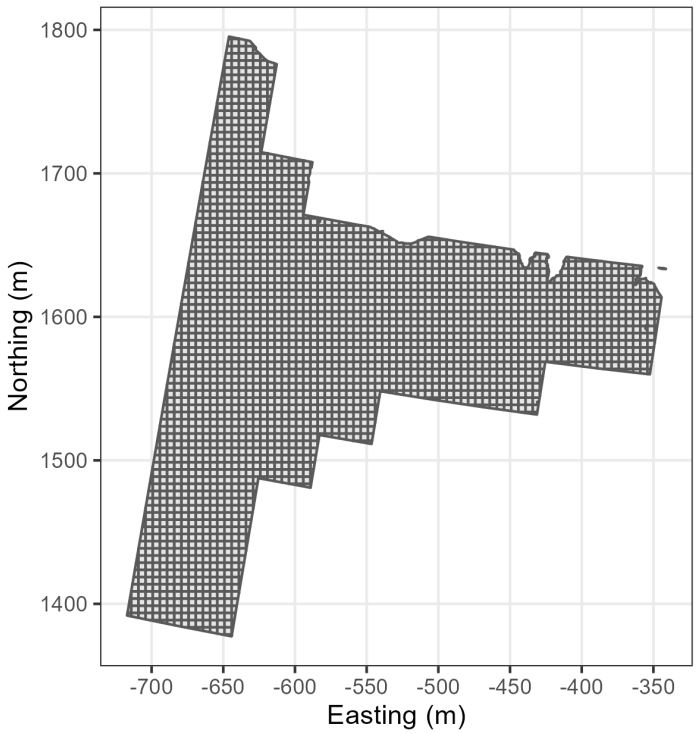


Figure 8: Prediction grid used to generate Norton Sound red king crab abundance estimates.

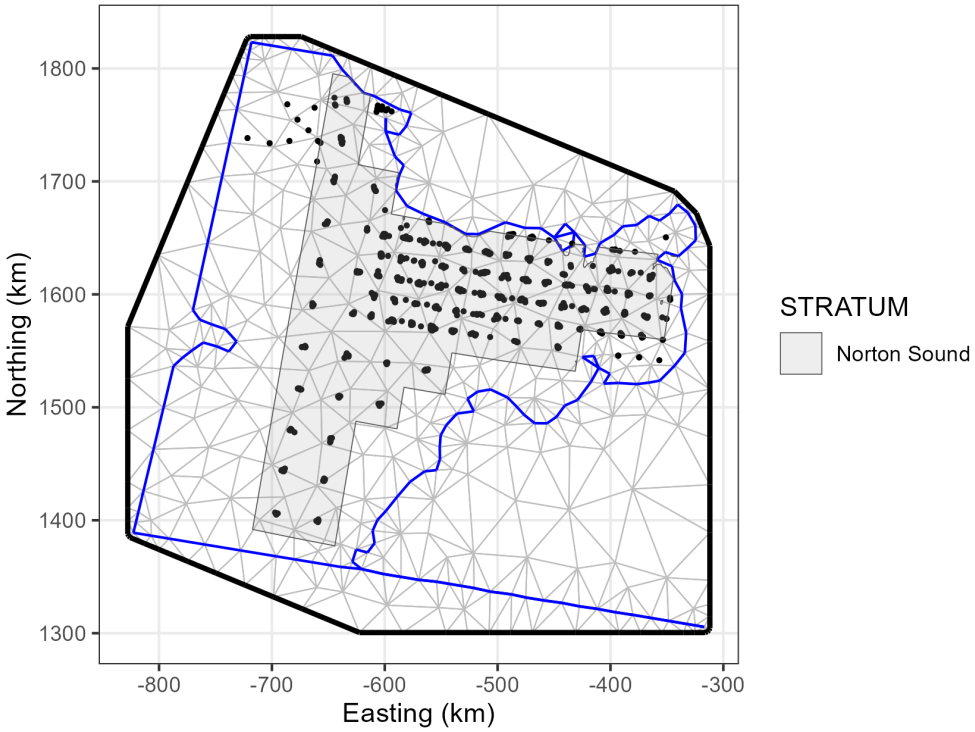


Figure 9: NOAA Northern Bering Sea bottom trawl survey stratum for the Norton Sound red king crab stock (light grey) overlaid on the spatial mesh used in spatiotemporal models, with ADFG and NOAA NBS survey observations shown as black points.

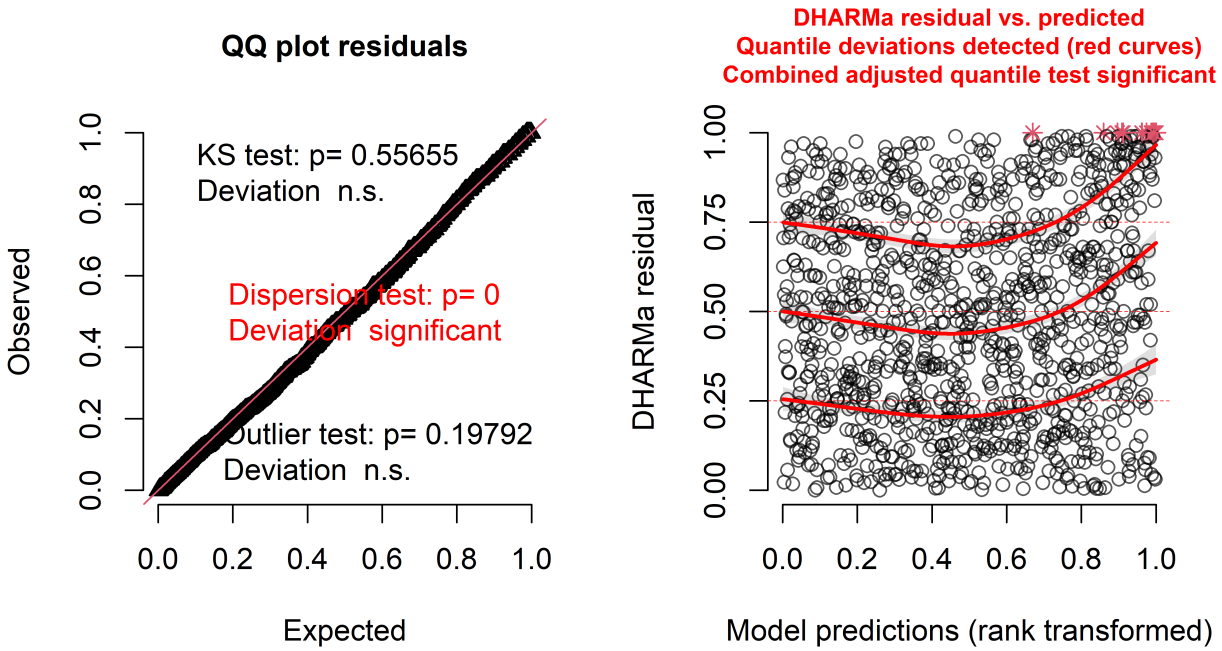


Figure 10: Diagnostics for the delta gamma distribution family model with year and survey as fixed effects, using DHARMa residuals.

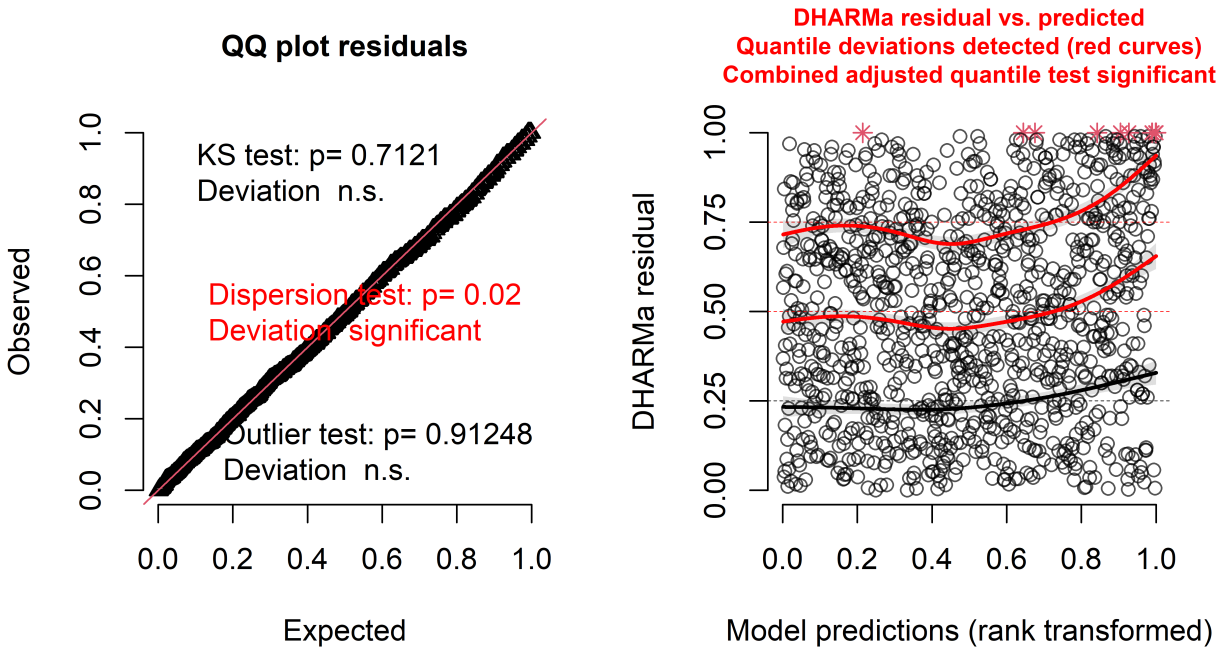


Figure 11: Diagnostics for the delta gamma distribution family model with year, survey, and depth as fixed effects, using DHARMa residuals.

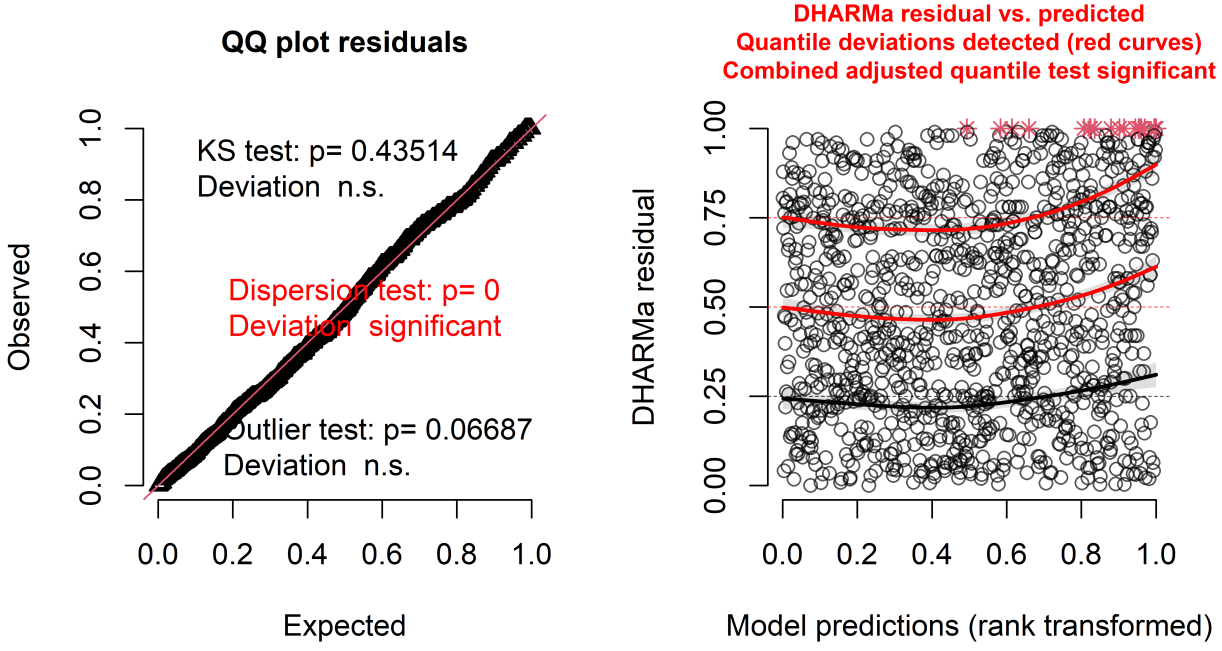


Figure 12: Diagnostics for the delta lognormal distribution family model with year and survey as fixed effects, using DHARMa residuals.

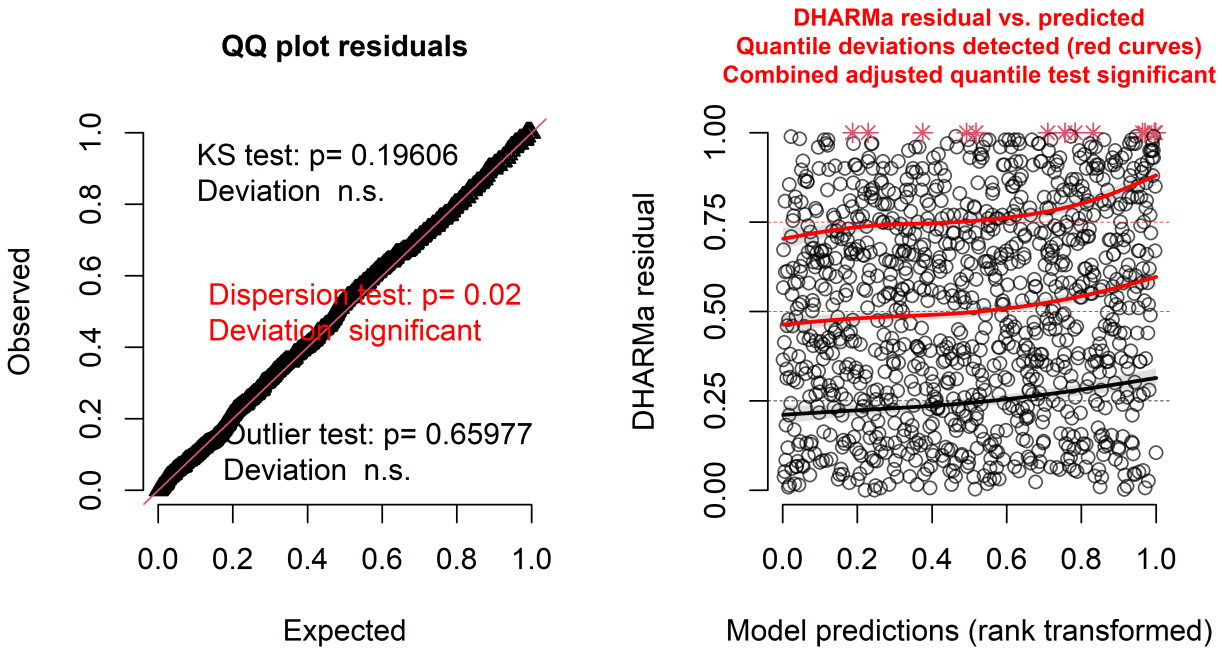


Figure 13: Diagnostics for the delta lognormal distribution family model with year, survey, and depth as fixed effects, using DHARMa residuals.

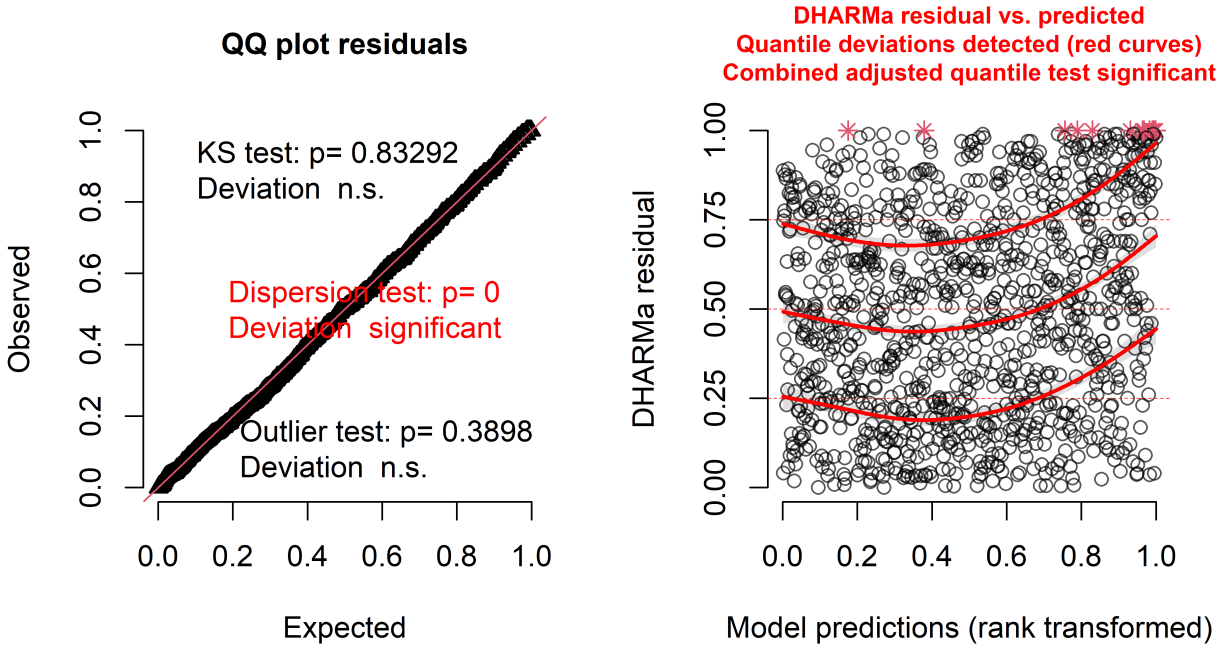


Figure 14: Diagnostics for the Tweedie distribution family model with year and survey as fixed effects, using DHARMa residuals.

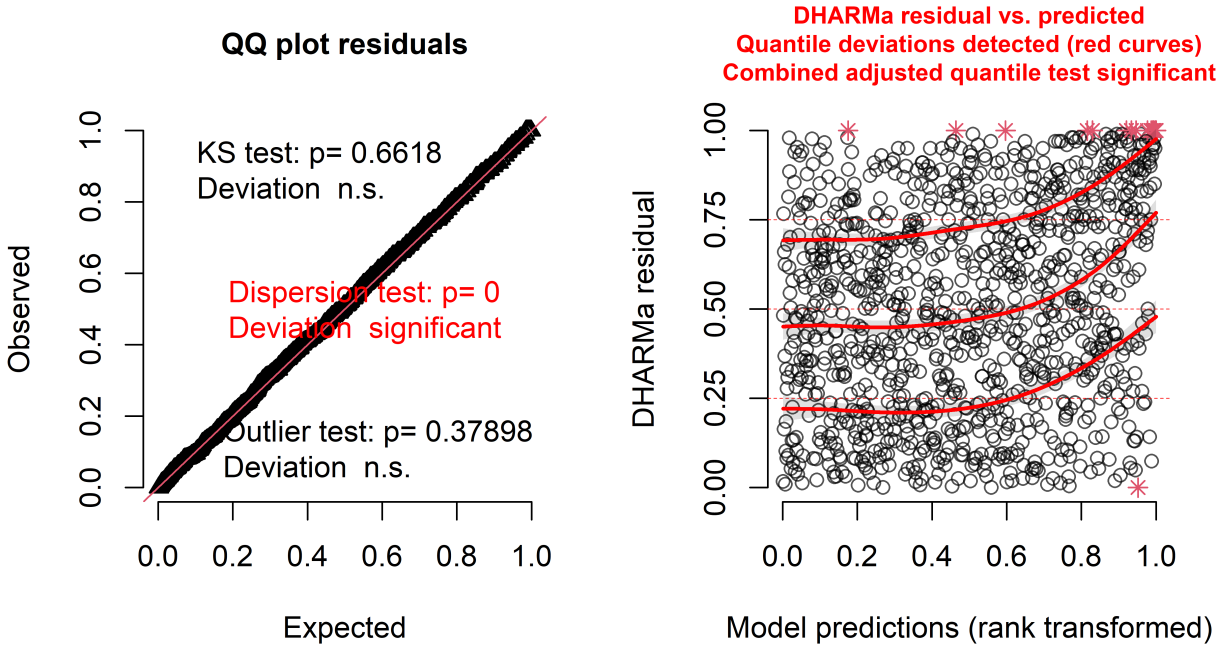


Figure 15: Diagnostics for the Tweedie distribution family model with year, survey, and depth as fixed effects, using DHARMa residuals.

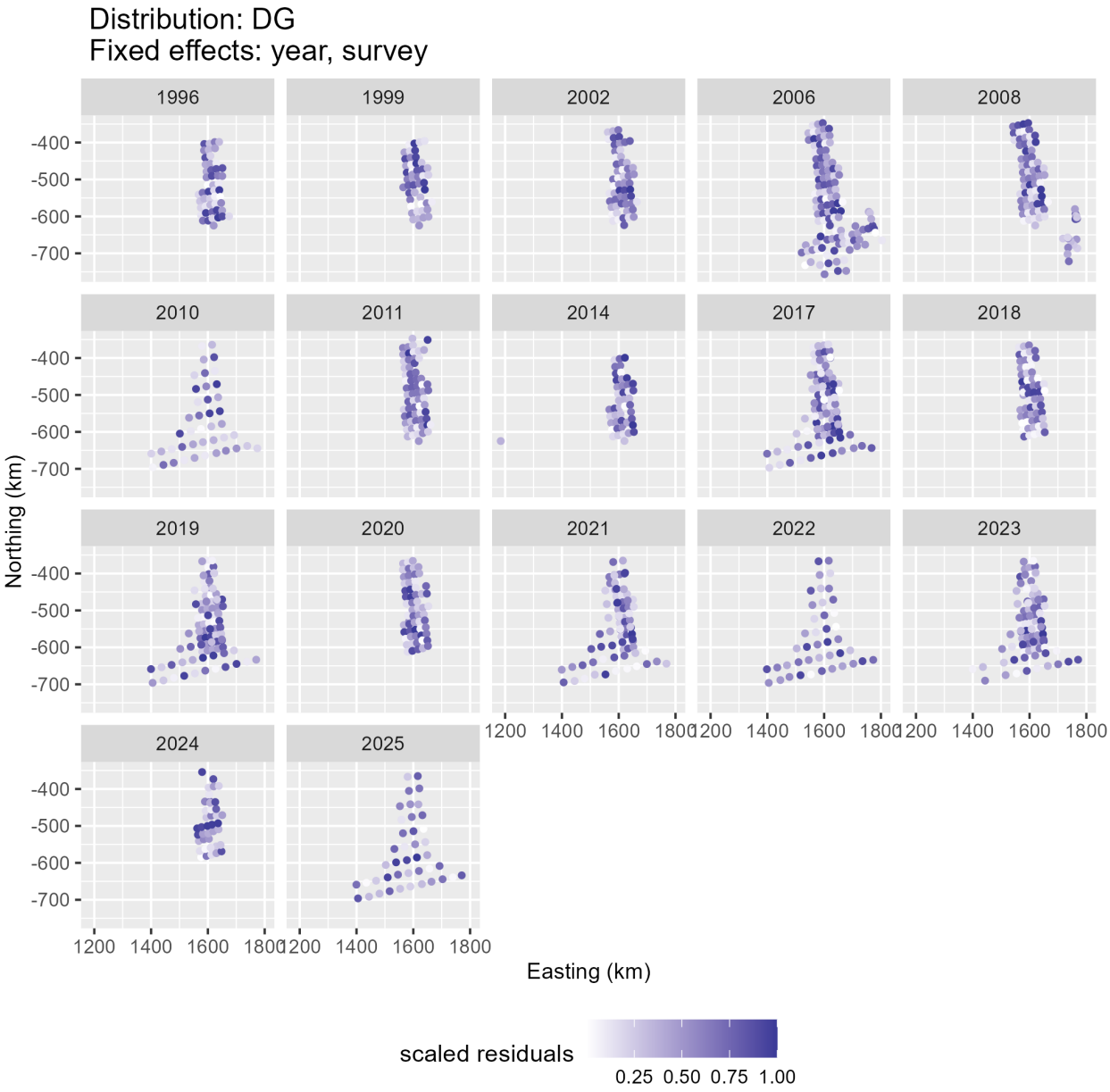


Figure 16: Spatial distribution of DHARMa residuals for the model using the delta gamma distribution with year and survey as fixed effects.

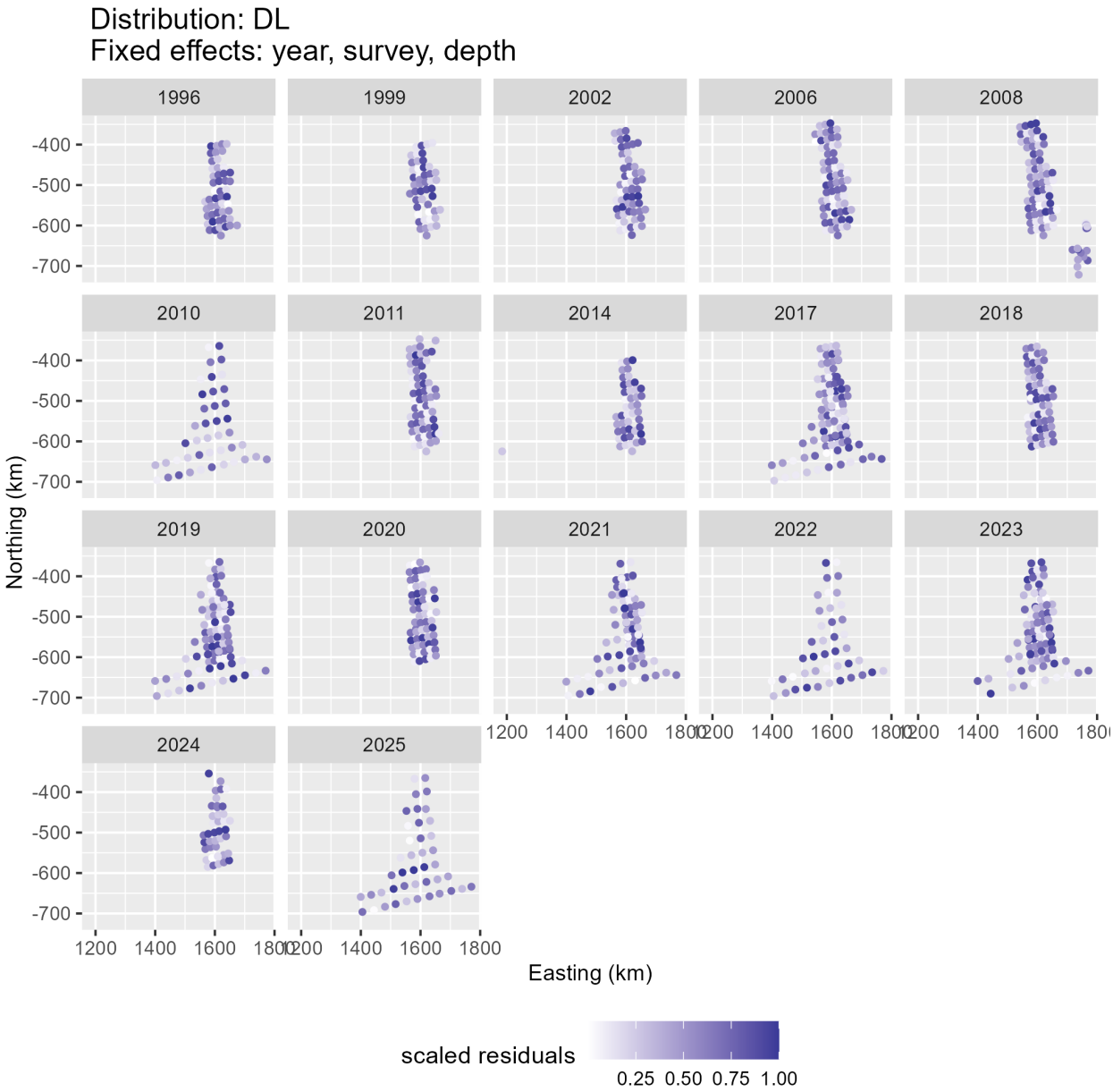


Figure 17: Spatial distribution of DHARMa residuals for the model using the delta lognormal distribution with year, survey, and depth as fixed effects.


Figure 18: Spatial distribution of DHARMa residuals for the model using the delta lognormal distribution with year and survey as fixed effects.

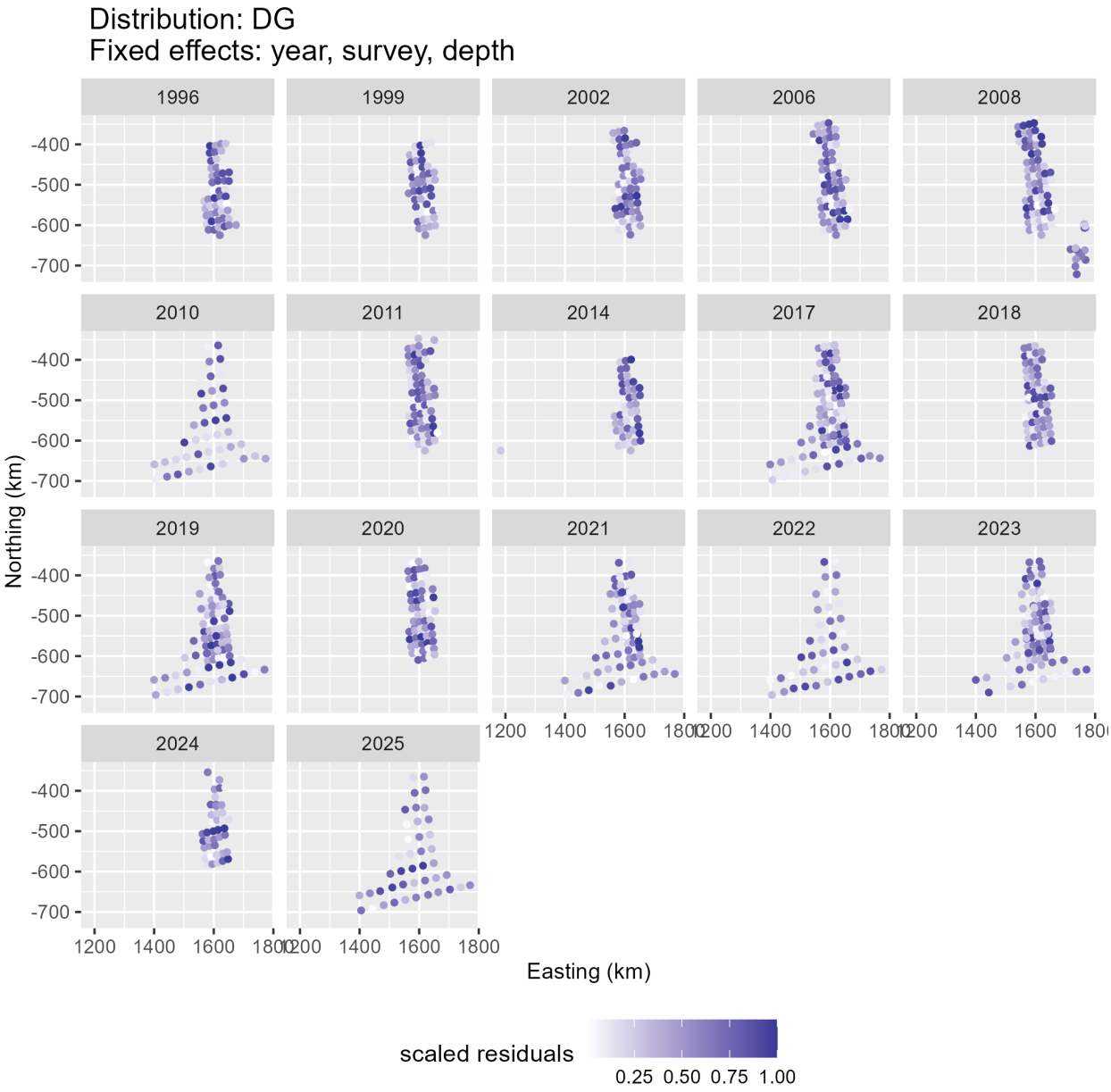


Figure 19: Spatial distribution of DHARMa residuals for the model using the delta gamma distribution with year, survey, and depth as fixed effects.

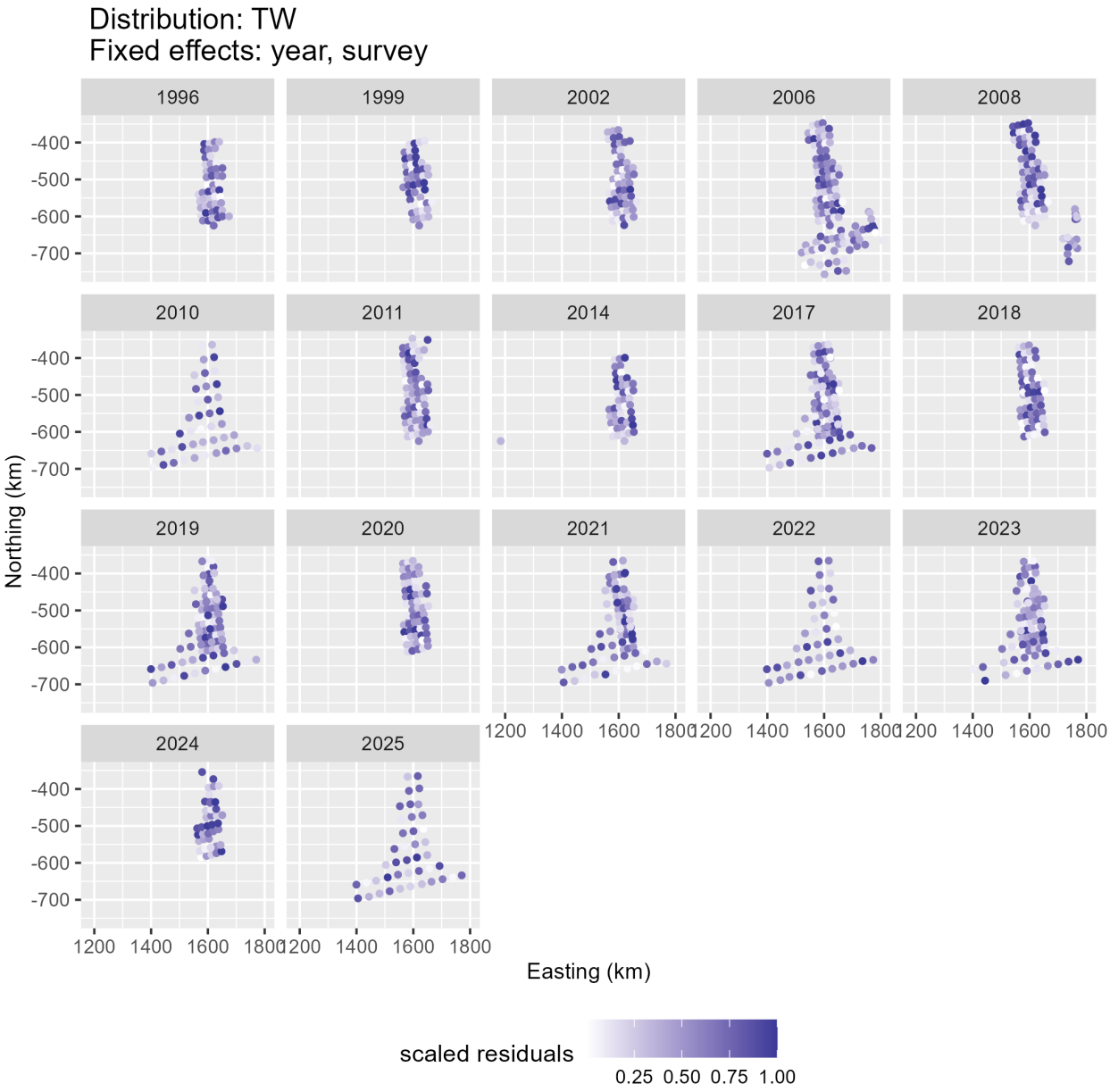


Figure 20: Spatial distribution of DHARMa residuals for the model using the Tweedie distribution with year and survey as fixed effects.

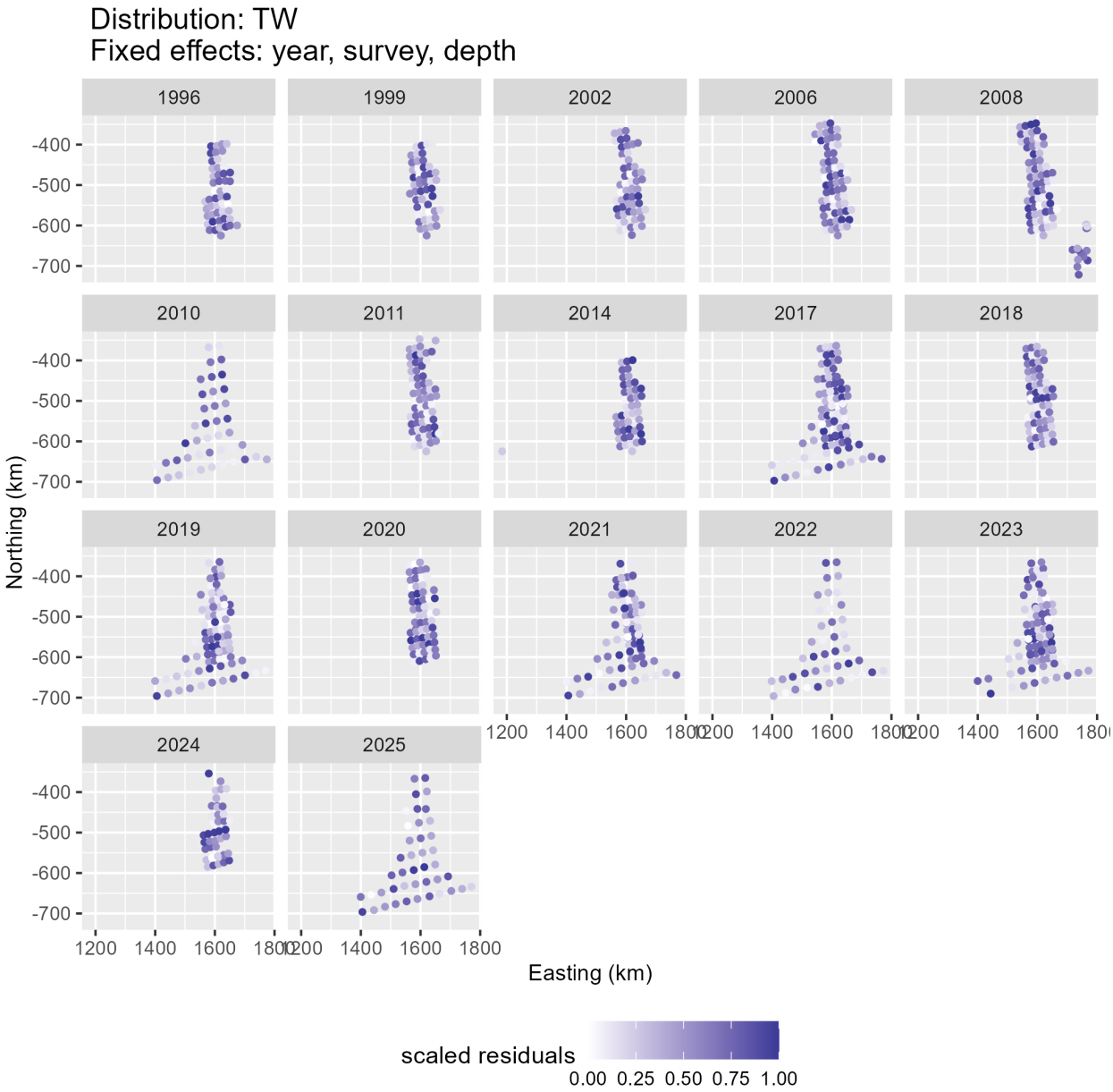


Figure 21: Spatial distribution of DHARMa residuals for the model using the Tweedie distribution with year, survey, and depth as fixed effects.

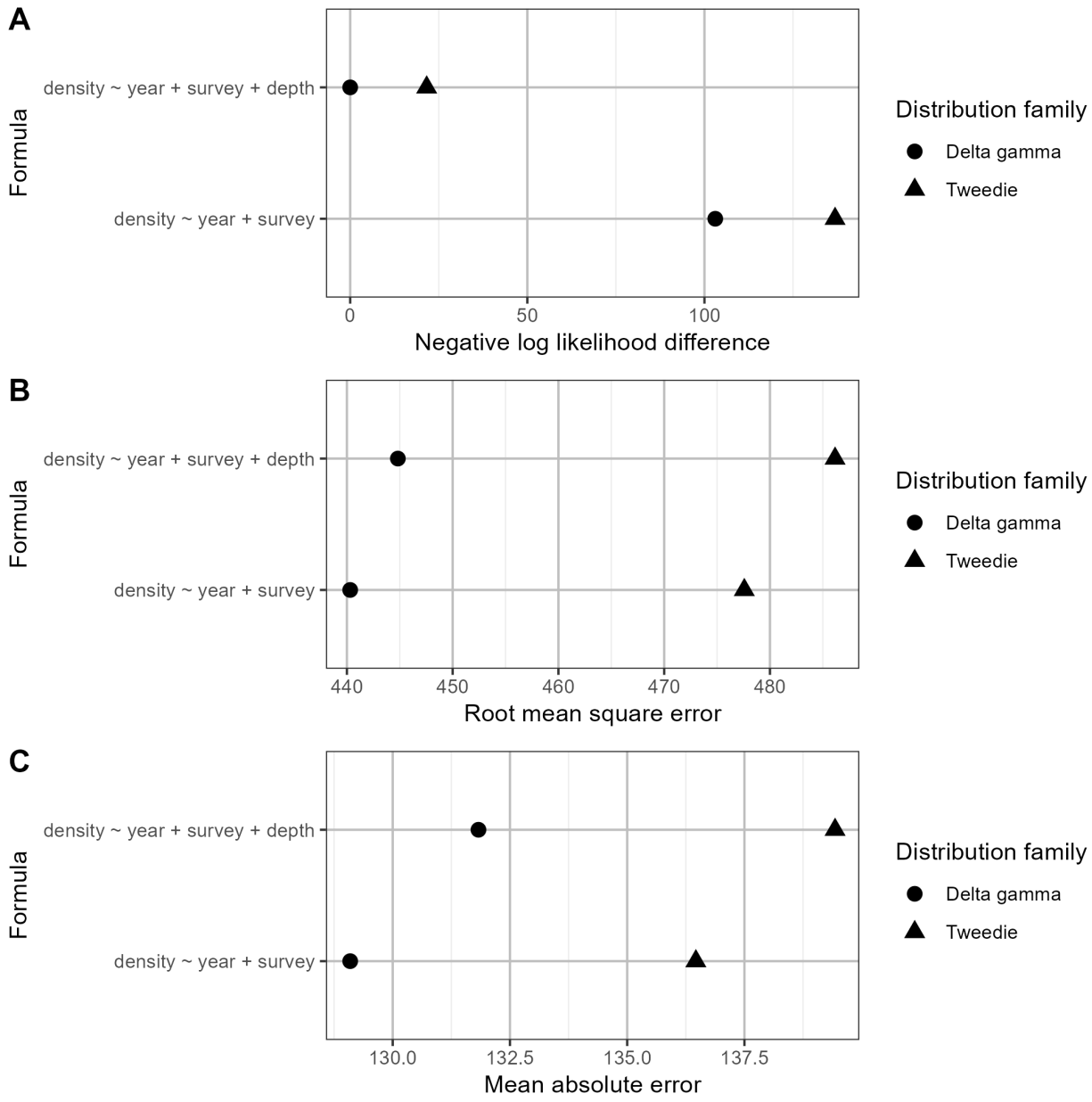


Figure 22: Metrics used in model selection, based on 10-fold cross validation. Note that models using the delta lognormal distribution family are not shown because, for each of those models, not all of the ten folds in the cross-validation analysis had non-positive-definite Hessian matrices. A) Negative log likelihood difference compared to the best-fitting model, which has NLL difference = 0, where smaller values indicate better model fit. B) Root mean square error, a measure of the average difference between observed and predicted values, where a lower value indicates better model fit. C) Mean absolute error, a measure of the average absolute value of the difference between observed and predicted values, where a lower value indicates better model fit.

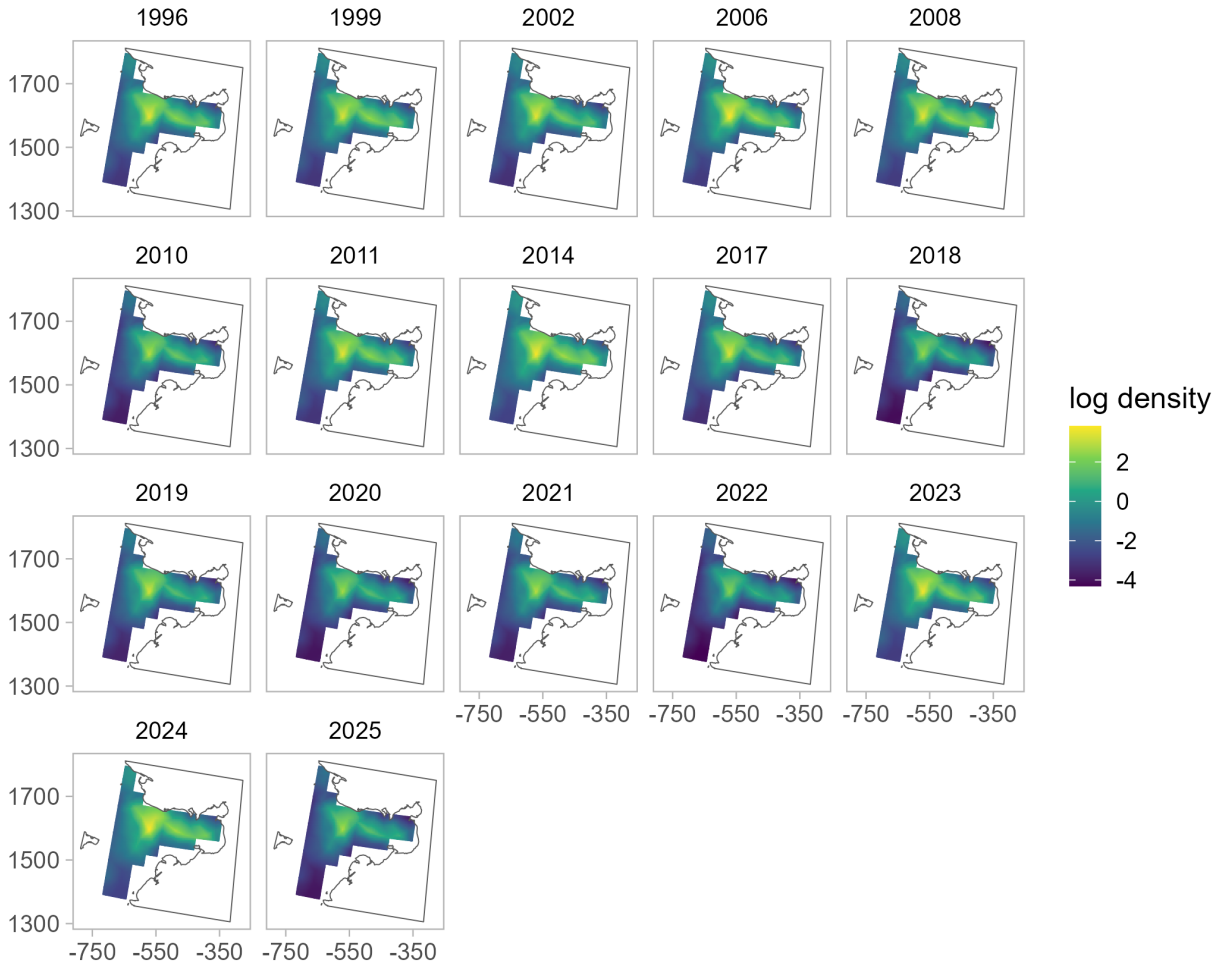


Figure 23: Spatial predictions of Norton Sound red king crab males $\geq$ 64 mm in carapace length by year from the model using the delta gamma distribution with year and survey as fixed effects. These predictions are from the presence/absence component of the hurdle model.

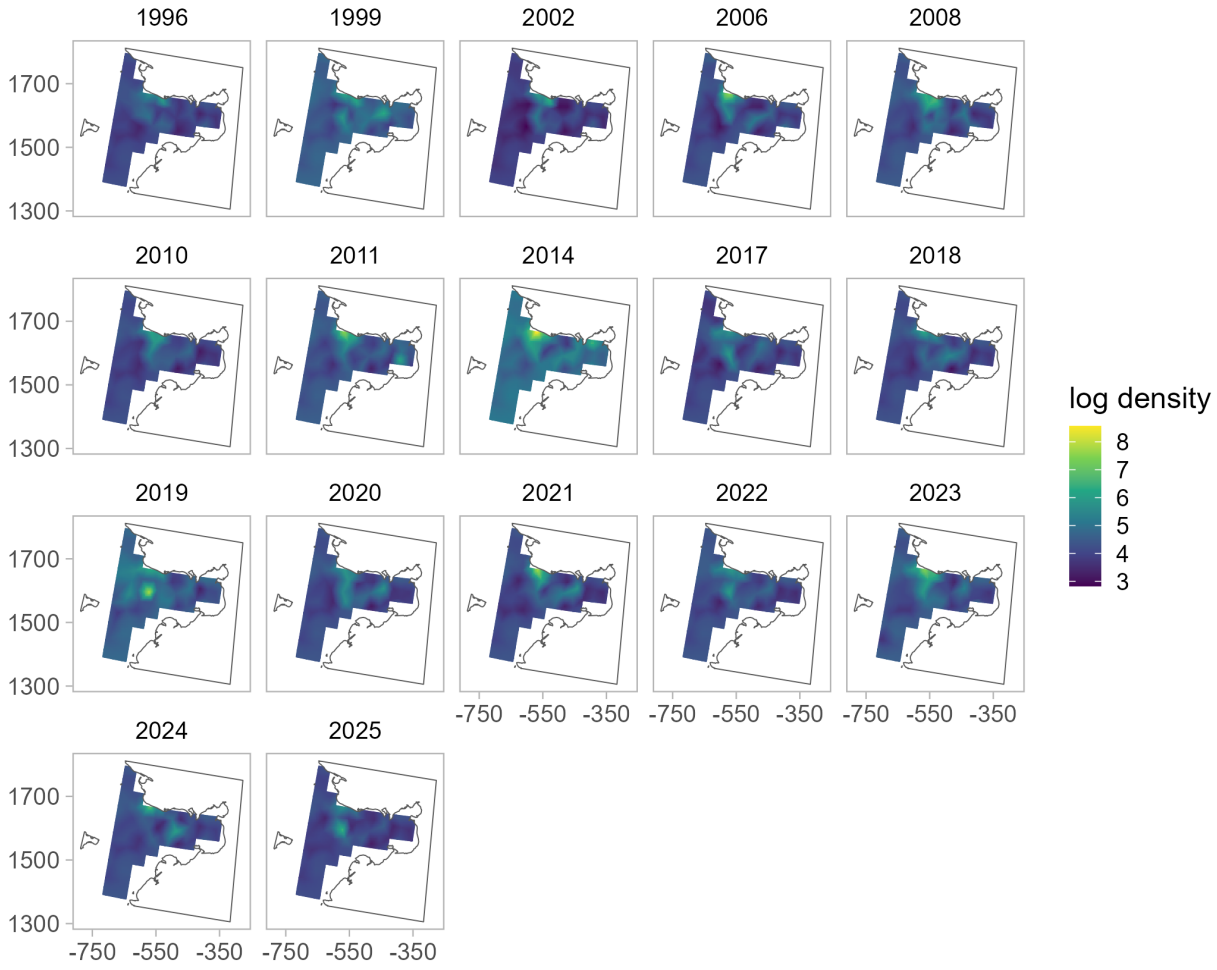


Figure 24: Spatial predictions of Norton Sound red king crab males $\geq$ 64 mm in carapace length by year from the model using the delta gamma distribution with year and survey as fixed effects. These predictions are from the positive catch (abundance) component of the hurdle model.

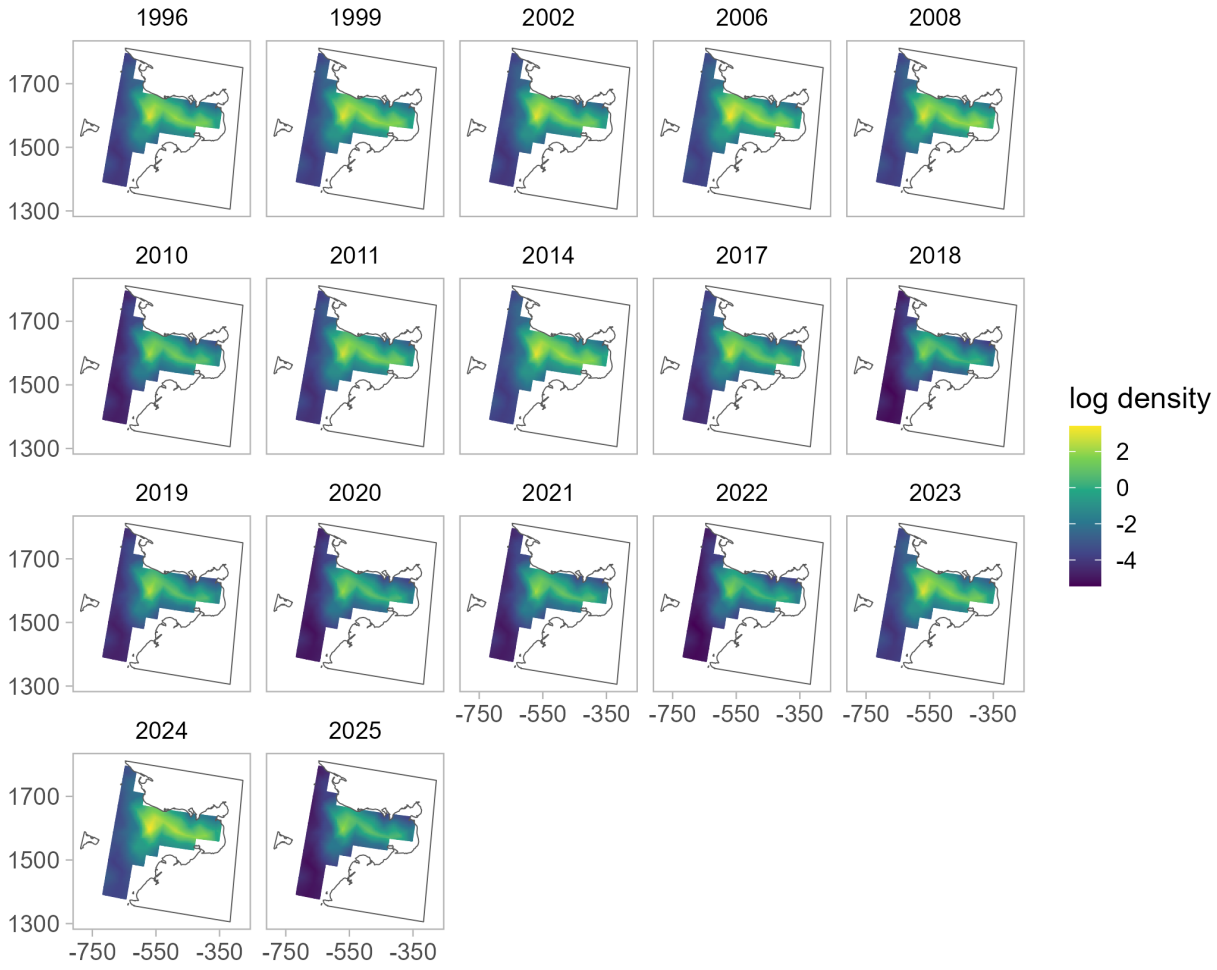


Figure 25: Spatial predictions of Norton Sound red king crab males $\geq$ 64 mm in carapace length by year from the model using the delta gamma distribution with year, survey, and depth as fixed effects. These predictions are from the presence/absence component of the hurdle model.

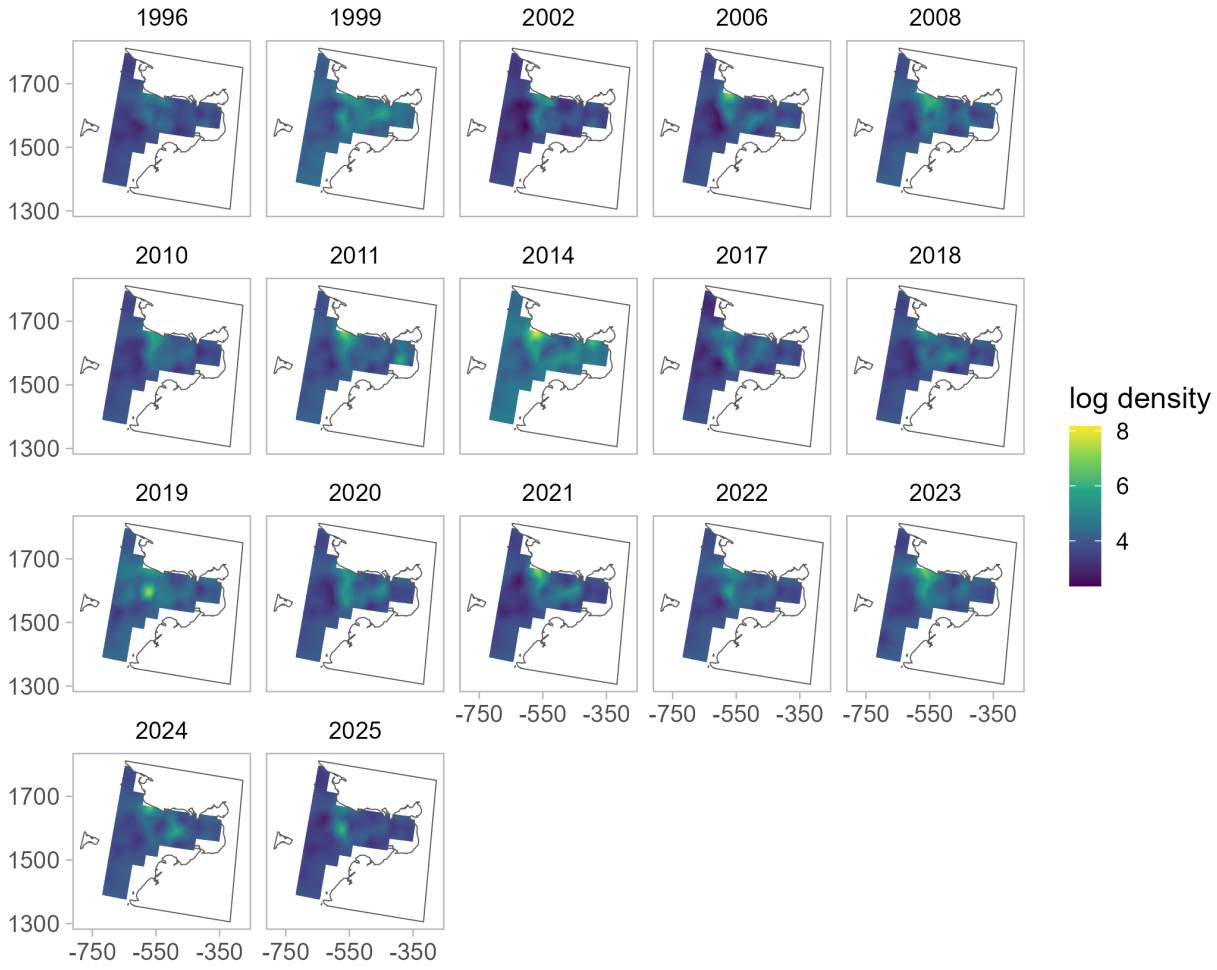


Figure 26: Spatial predictions of Norton Sound red king crab males $\geq$ 64 mm in carapace length by year from the model using the delta gamma distribution with year, survey, and depth as fixed effects. These predictions are from the positive catch (abundance) component of the hurdle model.

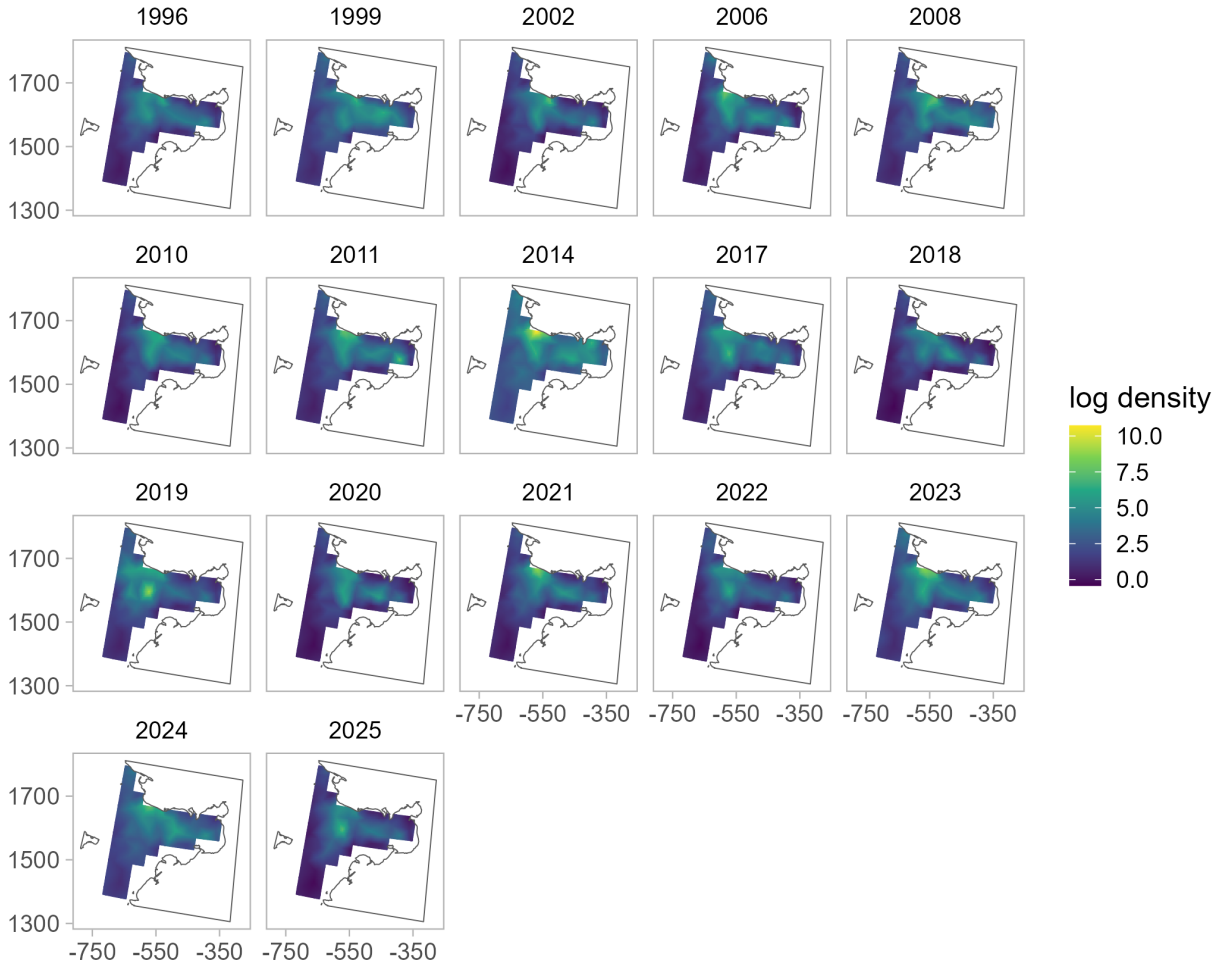


Figure 27: Spatial predictions of Norton Sound red king crab males $\geq$ 64 mm in carapace length by year from the model using the Tweedie distribution with year and survey as fixed effects.

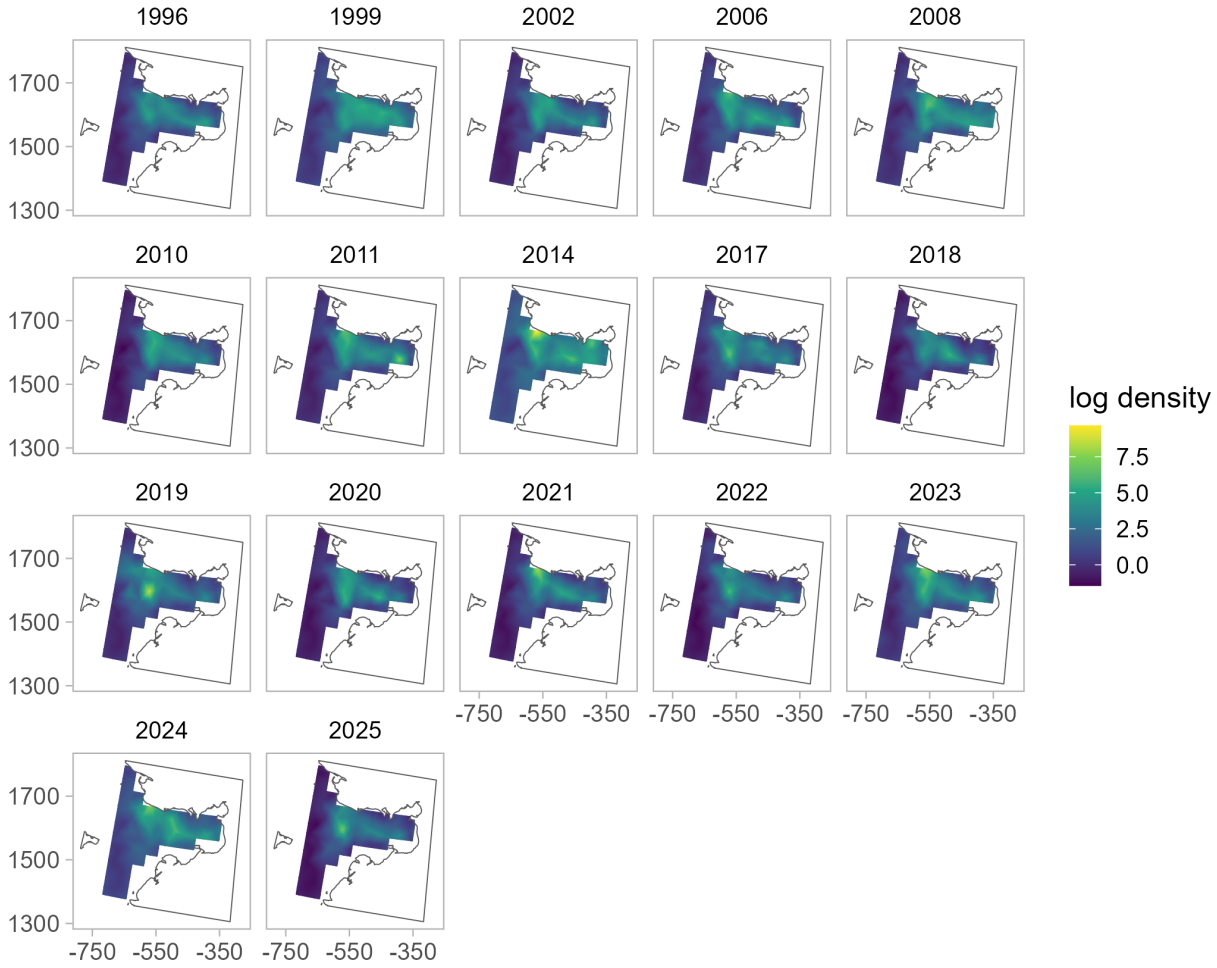


Figure 28: Spatial predictions of Norton Sound red king crab males $\geq$ 64 mm in carapace length by year from the model using the Tweedie distribution with year, survey, and depth as fixed effects.

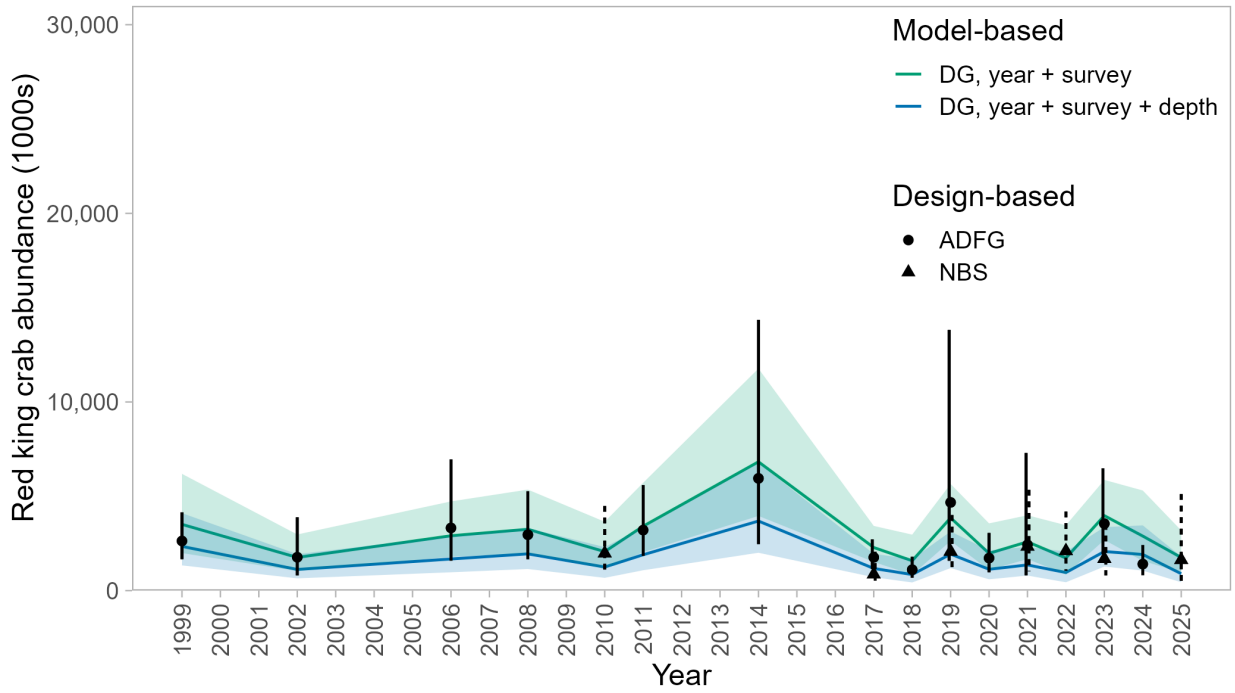


Figure 29: Estimated Norton Sound red king crab abundance for males with carapace length $\geq$ 64 mm. Colored lines represent abundance ($\pm$95% CI) estimated using spatiotemporal models with the delta gamma distribution family and fixed effects year and survey (green) or fixed effects year, survey, and depth (blue). Black points represent design-based abundance ($\pm$95% CI) estimates currently used in the stock assessment model from the NOAA Northern Bering Sea trawl survey (triangles, dashed error bars) and the ADFG trawl survey (circles, solid error bars).

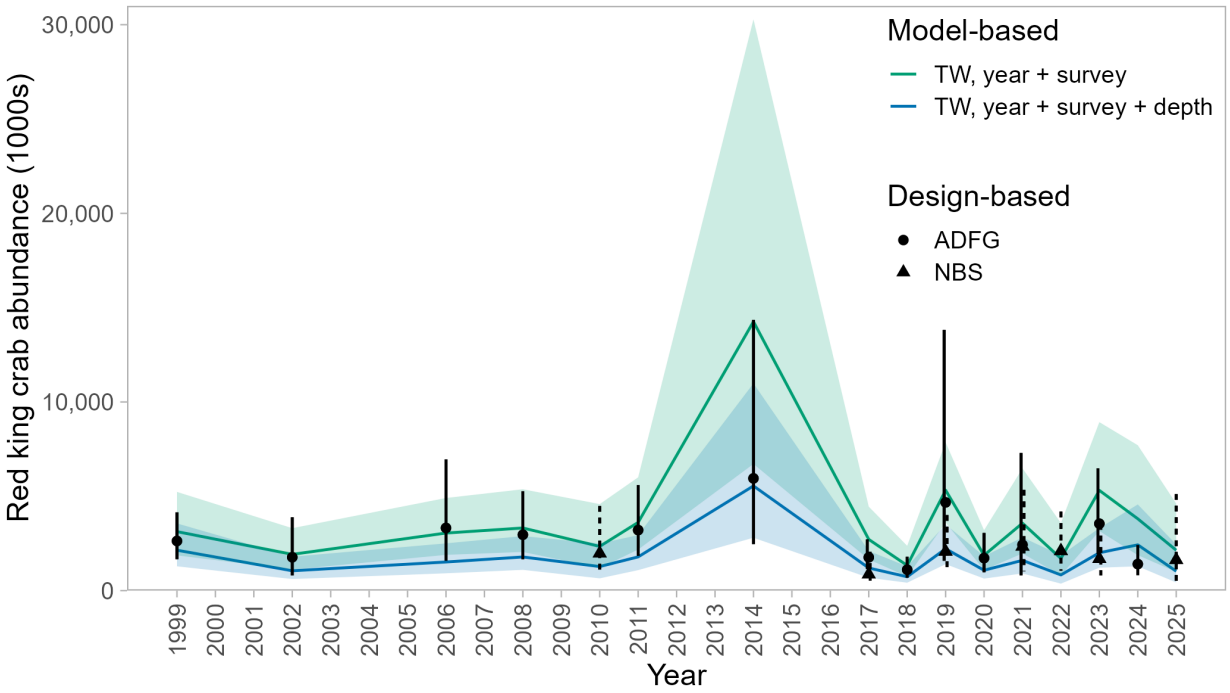


Figure 30: Estimated Norton Sound red king crab abundance for males with carapace length $\geq$ 64 mm. Colored lines represent abundance ($\pm$95% CI) estimated using spatiotemporal models with the Tweedie distribution family and fixed effects year and survey (green) or fixed effects year, survey, and depth (blue). Black points represent design-based abundance ($\pm$95% CI) estimates currently used in the stock assessment model from the NOAA Northern Bering Sea trawl survey (triangles, dashed error bars) and the ADFG trawl survey (circles, solid error bars).